


Active fault database of Turkey

Ömer Emre¹  · Tamer Y. Duman¹ · Selim Özalp² ·
Fuat Şaroğlu³ · Şeyda Olgun² · Hasan Elmacı² ·
Tolga Çan⁴

Received: 4 May 2016 / Accepted: 24 October 2016 / Published online: 10 December 2016
© Springer Science+Business Media Dordrecht 2016

Abstract We have updated the active fault map of Turkey and built its database within GIS environment. In the study, four distinct active fault types, classified according to geochronological criteria and character, were delineated on the 1:25,000 base map of Turkey. 176 fault segments not included in the former active fault map of Turkey, have been identified and documented. We infer that there are 485 single fault segments which are substantially potential seismic sources. In total 1964 active-fault base-maps were transferred into the GIS environment. Each fault was attributed with key parameters such as class, activity, type, length, trend, and attitude of fault plane. The fault parameters are also supported by slip-rate and seismogenic depth inferred from available GPS,

✉ Ömer Emre
o.emre@fugro.com

Tamer Y. Duman
t.duman@fugro.com

Selim Özalp
selim.ozalp@mta.gov.tr

Fuat Şaroğlu
fuat.saroglu@gmail.com

Şeyda Olgun
seyda.olgun@mta.gov.tr

Hasan Elmacı
hasan.elmaci@mta.gov.tr

Tolga Çan
tolgacan@cukurova.edu.tr

¹ Fugro Sial Geosciences Consulting and Engineering, Farabi Sok. 40/4, 06680 Çankaya, Ankara, Turkey

² Department of Geological Research, General Directorate of Mineral Research and Exploration, 06800 Çankaya, Ankara, Turkey

³ Magtur A.Ş., Çankaya, Ankara, Turkey

⁴ Department of Geological Engineering, Çukurova University, 01330 Adana, Turkey

seismological and paleoseismological data. Additionally, expected maximum magnitude for each fault segment was estimated by empirical equations. We present the database in a parametric catalogue of fault segments to be of interest in earthquake engineering and seismotectonics. The study provides essential geological and seismological inputs for regional seismic hazard analysis of all over Turkey and its vicinity.

Keywords Turkey · Active fault · Fault parameters · Seismic hazard

1 Introduction

Turkey is located in the Eastern Mediterranean region of Alpine–Himalayan orogenic system, which is one of the seismically most active zones in the world. Between 1900 and 2012, 203 earthquakes with magnitude of M_w 6.0 or greater were recorded within Turkey and the surrounding region (Kadirioğlu et al. 2016). The most destructive 72 of these earthquakes caused more than 90,000 casualties and imposed estimated economic losses (primary and secondary), of more than 50 billion dollars on the Turkish economy. The psycho-sociological impact of these earthquakes has been immense and last longer than the economic losses.

Seismic hazard maps are essential for many public policy applications in seismic hazard assessments and are an important component of seismic-design regulations for engineering structures. For that reason, these maps should be systematically updated and improved by the new seismic source data and assessments methods (Stirling et al. 2012; Rezaeian et al. 2014; Petersen et al. 2008, 2014a, b). Fault source models are a critical input to seismic hazard assessments (Litchfield et al. 2014).

The Active Fault Map of Turkey (1:1,000,000 scale; Şaroğlu et al. 1992a, b), which was the first map using consistent standards to document the essential characteristics of active faults on a national-wide scale, was published by the General Directorate of Mineral Research and Exploration (MTA). A range of earth science disciplines, planners, and engineers involved in the active tectonics and seismicity of Turkey and its surroundings have considerably benefited from the 1992 edition map.

Since 1992, geological and paleoseismological investigations on the earthquakes in Turkey (and around the world) have significantly increased. Additionally, two of most destructive earthquakes in history of Turkey, which are the 1999 İzmit (M_w 7.4) and Düzce (M_w 7.2) earthquakes (e.g. Barka et al. 2002; Duman et al. 2005), occurred providing valuable data that help to more fully understand Turkey's active faults and earthquake hazards for geoscientists. The last events and accompanying knowledge highlighted the need for more reliable and detailed active fault maps to support future scientific activities, to understand earthquake hazards, and to mitigate the risk from future seismic events. In recognition of the need for an updated active fault map for seismic hazard assessment, the project entitled “updating the Active Fault Map of Turkey and its Database” was launched by the MTA in 2004 and completed in 2011.

The aim of this paper is to describe the active fault classification method and to summarize the active faults parameters in Turkey with their geometric continuations to cross-border seismic sources. Therefore, all active faults presented in this study were mapped in detail at a base scale of 1:25,000 and essential inputs for seismic hazard analysis for 485 fault segments were estimated. In total, 1964 active fault base maps were transferred into

Geographic Information System (GIS) environment to create an active fault database of Turkey. The database includes basic information such as fault and segment name, activity class, type, length, trend, and attitude of fault plane. The parameters are augmented by slip-rate and seismogenic depth inferred from published GPS, seismological and paleoseismological documents, and expected maximum magnitude estimated from empirical equations. We present the database of updated active fault maps of Turkey as basic information for assessment of earthquake hazard, research, planning and implementation studies all over the country and the surrounding area.

2 Active tectonic framework of Turkey

Earthquakes that have impacted Turkey are generated by the most important active faults of the Eastern Mediterranean region. The Eastern Mediterranean is a region of complex tectonics associated with the interaction of three major lithospheric plates—Eurasian, Arabian and African. Therefore, a better understanding of Turkey's seismicity requires a description of the active tectonics and deformation styles associated with plate interaction in the region.

Turkey comprises many lithospheric fragments that were derived from the major plate margins and then amalgamated during the Alpine orogeny (e.g. Ketin 1966; Şengör and Yılmaz 1981; Okay and Tüysüz 1999; Bozkurt and Mittweide 2001). It is characterized by actively deforming terrain resulting from post-collisional intra-continental convergence and tectonic escape. These phenomena are related to the closure of the Neotethys Ocean, collision of the Arabian and African plates with Eurasian plate and formation of the Anatolian micro-plate, which represent the Late Tertiary tectonic history of the Eastern Mediterranean region.

In the easternmost part of the Turkey, the southern branch of the Neotethyan Ocean was consumed by the northward collision of the Arabian plate with the Eurasian plate during Mid-Miocene time ~ 12 Ma (McKenzie 1972). The Arabian and Eurasian plates were eventually sutured together along the Bitlis–Zagros belt once the former oceanic crust was consumed (Şengör and Yılmaz 1981).

A greater portion of Anatolia resembled a low-land terrain dominated by peneplain morphology before the continental collision throughout Eastern Anatolia in Oligocene—Middle Miocene (Erinç 1953; Erol 1983). Due to the collision, the continental crust in Eastern Anatolia contracted while thickening. As a result of the overall uplift, eventually, the region transformed into a high-land by tectonic relief inversion (Şengör and Kid 1979; Şengör 1980; Şengör et al. 1985). Because of the inadequacy of the existing tectonic structures to compensate such crustal thickening by north–south compression, Anatolian plate started to form, and two plate bounding transform fault systems emerged—the right-lateral North Anatolian Fault (NAF) and the left-lateral East Anatolian Fault (EAF). The Anatolian micro-plate which is situated between these two transform faults initiated its westward movement in the Early Pliocene (~ 5 Ma) (e.g. Şengör 1979a, b, 1980; Şengör et al. 1985; Bozkurt 2001). As a result, the collision began to drive internal deformation and forced a large part of Turkey westwards through a process called extrusion tectonics or escape tectonics (Burke and Şengör 1986; Dewey et al. 1986; Şengör 1979a, b, 1980; Şengör and Kid 1979; Şengör et al. 1985; Armijo et al. 1999). Sub-neotectonic regions, which are characterized by discrete tectonic structures and processes were formed within

the timespan of this new tectonic period (Şengör et al. 1985; Barka and Reilinger 1997; Koçyiğit and Özacar 2003).

As for the recent tectonic processes in the region, Eastern Anatolia—situated between the Caucasus and the Bitlis–Zagros thrust belt—is being deformed under the north–south compressional tectonic regime. Recent crustal deformations in the region are compensated by faults with various geometries and mechanisms (Şaroğlu and Güner 1981; Şaroğlu 1985; Şengör et al. 1985). These include NE–SW oriented left-lateral, NW–SE oriented right-lateral conjugate strike-slip faults, N–S extending normal faults and extension fissures, and E–W trending folds, thrusts and reverse faults. While rotating counter-clockwise, the Anatolian plate moves westward between the NAF and EAF and southwestward thrusts on to the African plate along the Aegean subduction zone (McKenzie 1972, 1978; Jackson and McKenzie 1984; Şengör 1979a, b, 1980; Şengör et al. 1985; Taymaz et al. 1991a, b; Le Pichon et al. 1995; Armijo et al. 1999). The neotectonic of Western Anatolia is characterized by east–west oriented horst-graben structures which identifies a N–S oriented extensional regime. The West Anatolia extensional neotectonic province is bounded by the Eskişehir–Tuzgölü fault zone on the east (Barka et al. 1995; Koçyiğit and Özacar 2003). Throughout Central Anatolia which is situated in-between the East Anatolia compressional and the West Anatolia extensional tectonic regimes, complex deformation by strike-slip, normal and reverse faults is observed.

The NAF and EAF transform faults which facilitate the westward escape of the Anatolian plate and its thrusting onto the African plate are the main structures of regional importance in the recent tectonics of the Eastern Mediterranean. These are intra-continental transform structures where the NAF emerged between the Anatolian and Eurasian blocks and the EAF emerged between the Anatolian and Arabian plates. The Dead Sea Transform Fault Zone, Hellenic Arc and Cyprus Arc are the other major active structures of the neotectonic framework of Turkey and the surrounding region (Fig. 1).

3 Active fault database of Turkey

The “Updating of Active Fault Map of Turkey and its Database” MTA project, included active fault investigations and 1:25,000 scale active fault mapping. All mapped active faults were digitized at 1:25,000 scale to and attributed with parametric data to create a GIS digital database. By the utilization of these data active fault maps at various scales were composed throughout Turkey. The methodology for the development of the active fault database and active fault map production summarized below.

3.1 Data source

The data presented in this paper includes active faults that were newly identified through aerial photo interpretations and field studies, or faults that were reinterpreted after the publication of the first Active Fault Map of Turkey (Şaroğlu et al. 1992a, b). Some of the faults were adopted partly from Şaroğlu et al. (1992a, b) and partly from later studies. The MTA Geological map database was used primarily to determine the age and offset-magnitude of the faults in the present active fault map.

Since there are no available standard data, the offshore extension of the faults or offshore faults were in general not included in the active fault maps. An exception was for the Sea of Marmara and Gulf of Saros, where a large amount of data were acquired after

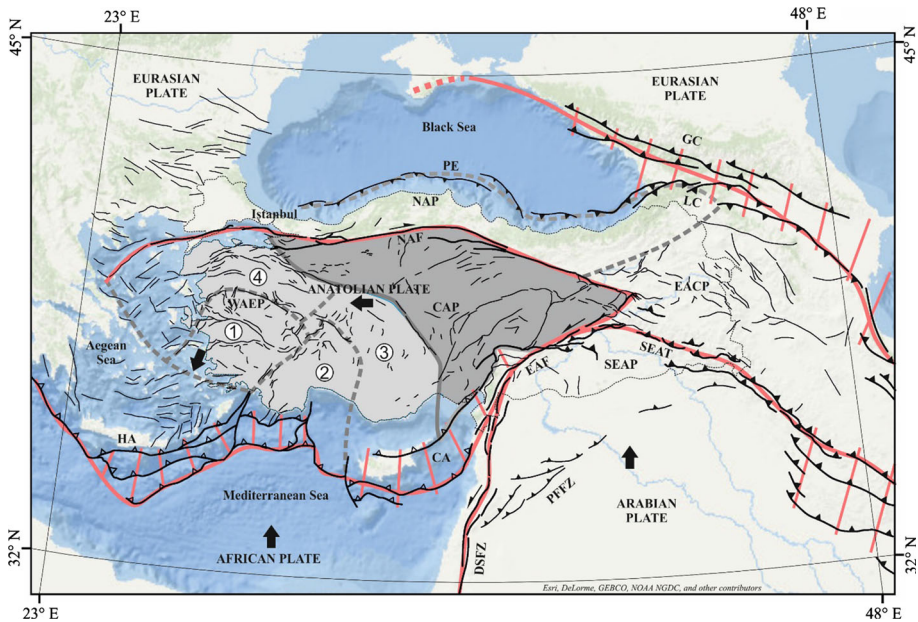


Fig. 1 Active fault map of the Eastern Mediterranean region and tectonic provinces. Faults in Turkey are from Emre et al. (2013). Faults in the south and east are simplified from Garfunkel (2014), Hessami et al. (2003) and Gudjabidze (2003). Faults in Aegean and Balkans are from Burchfiel et al. (2006), Caputo et al. (2012, 2015), Woessner et al. (2015). Faults in Mediterranean are re-evaluated from Angelier et al. (1982) and Papazachos and Papaioannou (1999). Faults in Black Sea are re-evaluated from Şengör et al. (1985) and Barka and Reilinger (1997). Neotectonic Province modified from Şengör (1980) and Koçyiğit and Özacar (2003). For the other details of the faults in Turkey see Fig. 3. HA Hellenic arc, CA Cyprian arc, DSFZ Dead Sea Fault Zone, EAFZ East Anatolian Fault Zone, NAFZ North Anatolian Fault Zone, SAITZ Southeast Anatolian Thrust Zone, PE Pontic Escarpment, LC Lesser Caucasus, GC Great Caucasus, WEAP West Anatolian Extensional Province: (1) West Anatolia graben systems, (2) Outer Isparta Angle, (3) Inner Isparta Angle, (4) Northwest Anatolia transition zone, CAP; Central Anatolian Province, EACP; East Anatolian Compressional Province, NAP; North Anatolian Province, SEAP; Southeast Anatolia Province, PPFZ; Palmyra Fault and Fold Zone. Subduction zones are shown by heavy lines with open triangles: the tips of triangles indicate polarity. Heavy lines with filled triangles at hanging wall indicate thrust zones. Heavy lines with half arrows are transform faults: the half arrows show relative movement along these faults. Lines with open triangles represent reverse fault zones. Bold arrows indicate the direction of plate motion. Thick hatched red lines show plate boundary fault zones. Thick dashed grey lines represent boundaries of major and sub-tectonic provinces

the 1999 İzmit earthquake to understand the nature of the offshore extension of the NAF. We reviewed these published data to delineate the underwater continuation of the NAF in Turkish territorial waters. The submarine parts of the NAF are interpreted after Rangin et al. (2001), İmren et al. (2001), Le Pichon et al. (2001, 2003), Armijo et al. (2002, 2005) Kuşçu et al. (2002), Cormier et al. (2006), İmren (2007) for the Sea of Marmara, and Ustaömer et al. (2008) for the Gulf of Saros, Koukouvelas and Aydın (2002) for the North Aegean Trough. Based on the references cited above only the Holocene underwater faults are included in the revised active fault maps. Additionally, available literature was used to evaluate the neotectonic setting, activity, slip rate and earthquake behaviour of the faults and their seismogenic depths.

3.2 Mapping methodology

The study was based on interpretations of 1:35,000- 1:20,000- and 1:10,000-scale aerial photos, ortophotos and digital terrain analysis produced from topographic maps of 10 m interval contours, and coupled with detailed field surveys. During the field surveys, fault and related features were observed and documented. These included information such as the structural origin, age, offset, segment and jog structures, and geological and geomorphological observations.

All these data were compiled into the 1:25,000 scale topographic maps. Then, these base maps were digitized into a GIS environment so that both analogue and digital archives of the particular fault map were created. Maps of each fault were then sequentially added to the database in a consistent format to create the active fault map series.

3.3 Nomenclature

The fault names are intended to be compatible with those used by Şaroğlu et al. (1992a, b) on the prior edition of the Active Fault Map of Turkey. However, new names were assigned to some faults that were identified or segmented in this study using the name of the closest major settlements shown on the 1:250,000 scale topographic maps of Turkey. In other literature, some of the faults are sometimes cited with different names or using local names such as a village, river or hill, etc. In these cases, we have also renamed the faults using the project's standards. On the other hand, if a particular part of a fault identified in the literature is actually a minor part of a larger fault zone then that minor fault was renamed to that of the greater fault system. Single names are used for the more or less geometrically single segment faults.

3.4 Definitions

The term 'fault zone' is used for a fault group that forms a zone where individual faults are parallel or semi-parallel to each other. The term "graben system" is reserved when multiple faults form or are located in a graben. The terms multi-segment fault, fault zone and fault system refer to large faults that are divided into segments and each identified segment is given a specific name.

The term 'segment' refers to the 'geometric segment' of McCalpin (1996), which is based on fault stepovers and bends. When available seismological and paleoseismological data are utilized in our study of segmentation, the segments defined may refer to the 'behavioural segment' of McCalpin (1996). The original 1:25,000 base map scale was selected so that fault geometry and segmentation of the faults could be represented by following the approaches of Knuepfer (1989), de Polo et al. (1989, 1991), and McCalpin (1996).

3.5 Classification

Classifications of active faults depend on neotectonic period and active tectonics of the terrain, available data and the scope of the study. The delineation of faults suggested by Jennings (1994) as; active faults, potentially active faults, and capable faults is very common, especially in nuclear power plant studies. We define an active fault as one that has produced a surface rupture in the Quaternary. The Quaternary is used as it falls within

the neotectonic period of Turkish territory which is considered to extend from the Late Miocene to present.

Surface deformations caused by earthquakes along the faults have long been used as the geological and geomorphological criterion for defining of active faults. We defined four distinct active fault types considering the time of the last surface rupture as the geochronological criterion and character (Fig. 2) classified the identified faults accordingly. The classes were defined as follows;

- (1) Fault with Earthquake Surface Rupture: A fault that produced a large magnitude earthquake after 1900, and where reliable data were available to document the rupture location and the total length of the surface rupture.
- (2) Holocene fault: A fault that has evidence of surface rupture during Holocene time (last 11,000 years).
- (3) Quaternary Fault: A fault that has evidence of surface rupture during Quaternary time (last 2588 million years).
- (4) Probable Quaternary fault or lineament: A fault with possible, but not definitive Quaternary activity. These faults may be associated with linear topographic features, which could be related to neotectonic or paleotectonic structures that control the present geomorphology. There is no clear evidence for surface rupture during Quaternary time.

3.6 Active fault maps of Turkey

We produced active fault map outputs at three different scales. These are; (1) Base maps of active fault at 1:25,000 scale, (2) Active fault map series of Turkey at 1:250,000 scale and (3) Active fault map of Turkey at 1:1,250,000 scale. The active fault base maps consist of 1964 sheets which were archived in both analogue and digital forms at the Geological Data Base of Turkey and the Map Archive of the MTA, respectively. These maps include data

Fault Class	Geological Time		Time (Year)	Tectonic Period	Activity
	Period	Epoch			
Earthquake surface rupture	Quaternary	Holocene	1900 – Recent	Neotectonic	Active
Holocene fault			11,000		
Quaternary fault		Pleistocene	2,588,000		Probable active
Lineament	Tertiary	Pliocene	5,000,000		
		Late Miocene	10,000,000	Inactive	
		Pre – Late Miocene			Paleotectonic

Fig. 2 Geological fault classification approach used in the Active Fault Maps of Turkey (Emre et al. 2013)

that can be used for regional seismic hazard analyses and surface fault rupture hazard analyses, as well as global route and site selection studies. However, the maps scales may be insufficient for project-specific studies, and these data are not a substitute for site-specific evaluations.

The base maps were then scaled to produce two primary products. The first is the 1:250,000 scale Active Fault Map of Turkey Series, consist of 59 individual sheets that were published between 2010 and 2012. References for all these sheets were listed in Emre et al. (2013). The second is the 1:1,250,000 scale Active Fault Maps of Turkey (Emre et al. 2013) which consists of a booklet with a map-appendix. This is a simplified guide map which shows the spatial distribution and general characteristics of the active faults in the Turkish territory.

The digital forms of the active fault maps in GIS environments are available to institutions, organizations and individuals for a particular fee. The active fault base maps including the detailed geometry are served on the Earth Science Map Portal of the MTA (<http://yerbilimleri.mta.gov.tr>). Additionally, all published maps, the Active Fault Map Series of Turkey (59 sheets) and the Active Fault map of Turkey are available at maps.mta.gov.tr in high resolution pdf format. Figure 3 shows the active fault distribution simplified from the Active Fault maps of Turkey.

4 Distribution of active faults and their regional characteristics

On the updated active fault maps of Turkey, there are 326 single faults, fault zones or systems. The large fault zone or systems were divided into segments based on their potential to produce earthquakes individually. Consequently, 485 single fault segments which are considerable potential seismic sources were identified across Turkey (Fig. 3).

Four distinct neotectonic provinces (Fig. 1) were suggested by Şengör (1979a, b) across Turkey: (1) North Anatolian province; (2) Eastern Anatolian contractional province; (3) Central Anatolian ‘Ova’ province; (4) Western Anatolian extensional province. Each province shows different tectonic characteristics. For example, the Eastern Anatolian region, between the Caucasus and the Bitlis–Zagros belt, is currently experiencing a N–S compressional tectonic regime, while Western Anatolia is deforming through N–S continental extension. Central Anatolia between these two regions is characterized by complex recent tectonic activity, expressed along strike-slip, normal and reverse faults (Koçyiğit and Özacar 2003). We modified the proposed models for neotectonic provinces of Turkey by Şengör (1980) and Koçyiğit and Özacar (2003) as shown in Fig. 1.

Within this general framework, our model suggests five distinct neotectonic provinces within Turkish territory. The Eastern Anatolian Province is under a S–N oriented compressional tectonic regime (Şengör 1980). The Anatolian plate moving westward in an escape tectonic regime is prominently divided into two neotectonic regions; (1) Central Anatolia to the east is dominantly characterized by strike-slip faulting mechanism due to pure lateral plate motion, (2) West Anatolia deforming under an extensional tectonic regime (Şengör 1980; Şengör et al. 1985). Both the Anatolian plate regions are divided into sub-divisions or blocs. Sub-provinces of the Western Anatolian extensional tectonic regime are shown in Fig. 1. The North Anatolian Province geologically corresponding to the Pontide orogenic belt including the Strandja massif at the west is situated between the Black Sea abyssal plain and plate boundary North Anatolian fault system (Fig. 1). The region is characterized by very low microseismicity (except for the 1968 Bartın

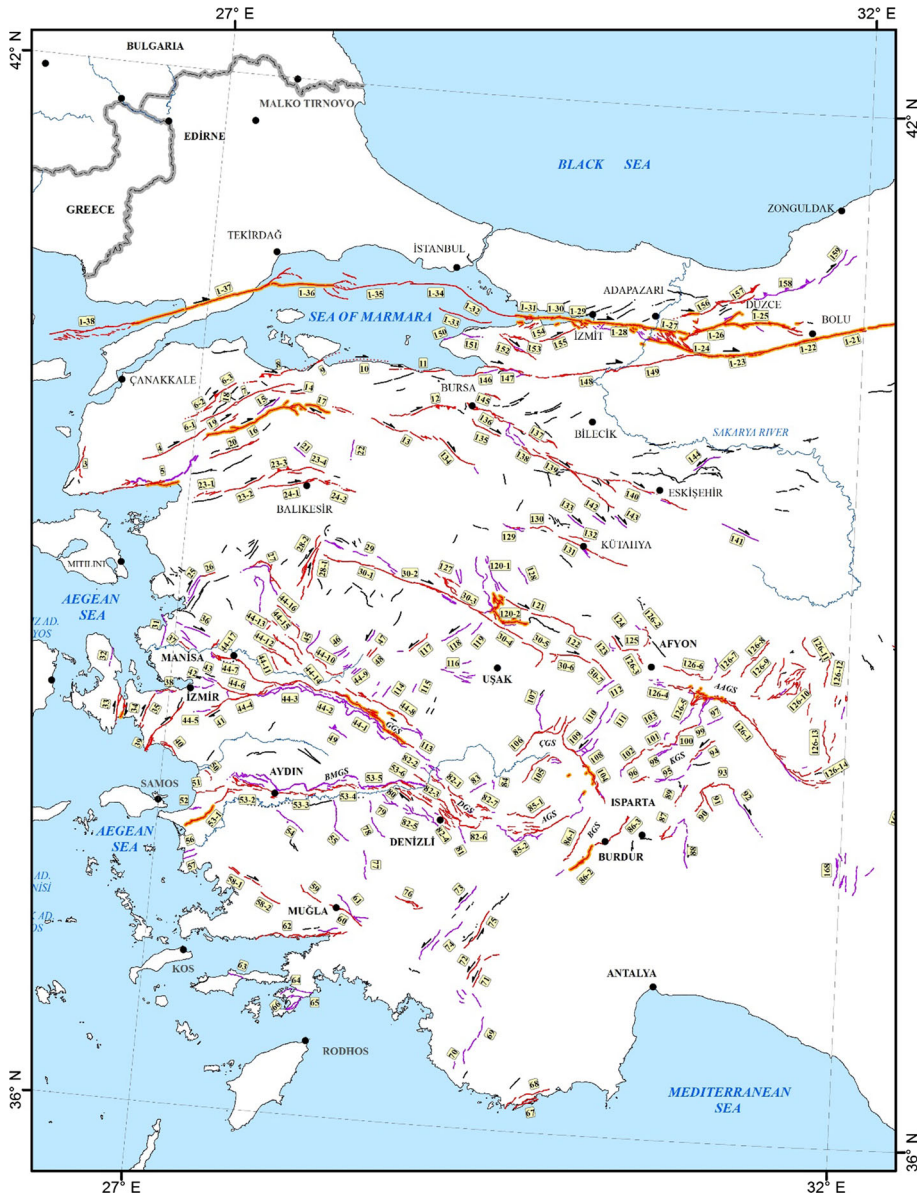


Fig. 3 Spatial distribution of the active faults of Turkey (3/3). Each fault or fault segment was defined by an *identification number*. The fault segments were numbered with sub class numbers. In this notation the *first number* shows that the fault has multi-segments, a fault system or a zone, the *second number* indicates the fault segment. The *identification numbers* of the faults associated with the names are in the Table 1. *BMGS* Büyük Menderes Graben System, *GGG* Gediz Graben System, *DGS* Denizli Graben System, *AGS* Acıgöl Graben System, *BGS* Burdur Graben System, *ÇGS* Çivril Graben system, *AAGS* Afyon-Akşehir Graben System, *KGS* Karamuk Graben System

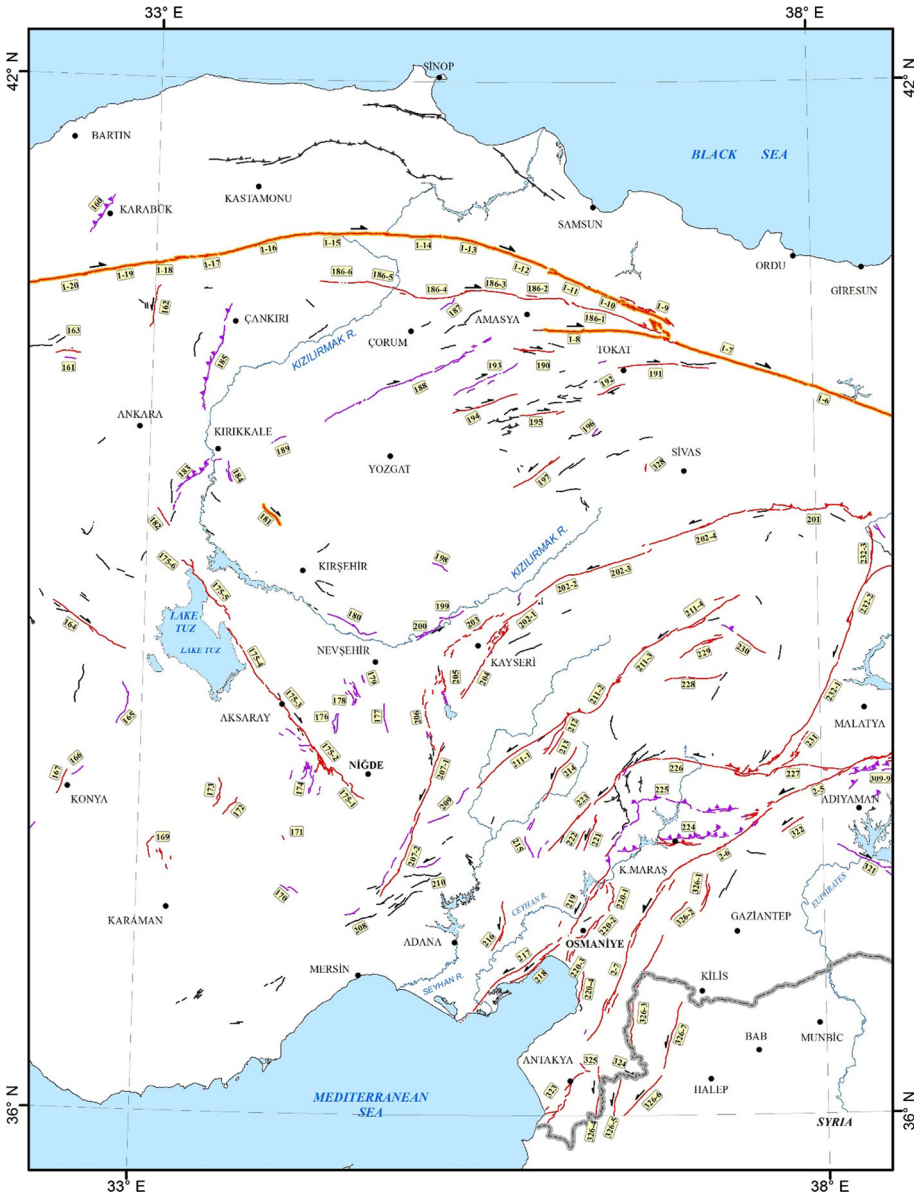


Fig. 3 continued

earthquake) and is bounded to the north by the Pontic Escarpment (Barka and Reilinger 1997) the Quaternary activity of which is still debated. Finally, the Southeast Anatolia province with scattered Quaternary faults the northern margin of Arabian plate represents the foreland along the Southeast Anatolian thrust zone. We recognized sub-provinces including faults that have similar geometries, kinematics and tectonic characteristics. The following section summarizes the information presented in the active fault maps of Turkey.

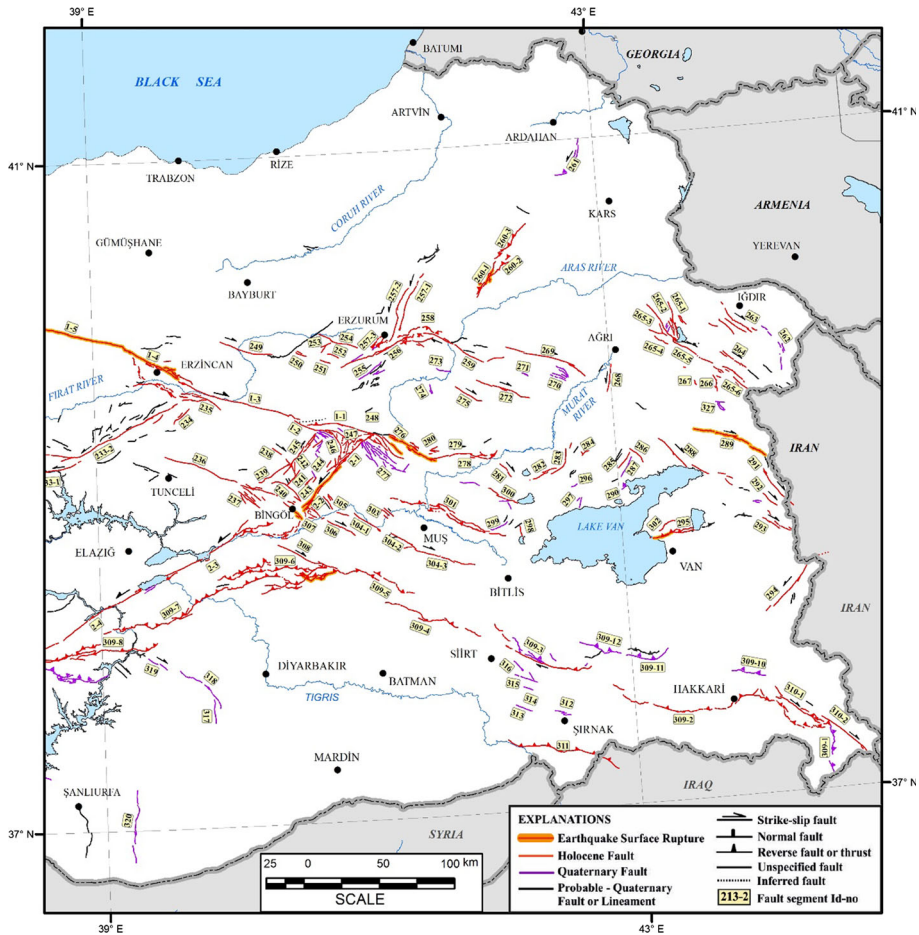


Fig. 3 continued

4.1 Plate boundary fault systems

4.1.1 The North Anatolian fault

The North Anatolian Fault (NAF) is a right-lateral strike-slip transform fault system which separates the Eurasian and Anatolian plates. The NAF zone, with its extraordinary morphological characteristics and its capacity for generating destructive earthquakes is one of the main active tectonic features of the Eastern Mediterranean region. Thus it has been subject to several investigations (Ketin 1948, 1968, 1969; Şengör 1979a, b; Şengör et al. 1985, 2005; Şaroğlu et al. 1992a, b; Barka 1992, 1996; Barka and Kadinsky-Cade 1988; Barka and Reilinger 1997; Koçyigit and Beyhan 1998; Bozkurt 2001 references therein; Emre et al. 2013 references therein). The NAF traverses E–W across Anatolia for ~1400 km starting from Karlıova to the north Aegean Sea.

Right-lateral geological offsets, fault valleys, tectonic troughs, offset ridges and drainage networks, pressure ridges of various sizes, basins and similar features along the fault

are identifier features of this transform fault (Şengör 1979a, b). Numerous basins with different dimensions which have developed due to the geometric relations are observed in the strike-slip zone along the NAF. Even though in detail these basins can be classified into different types a majority of them are jog structures which have developed in releasing bends or stepover areas. Erzincan, Niksar, Yeniçağa, Bolu, Düzce, Adapazarı, Lake Sapanca and several basins in the Sea of Marmara and the Gulf of Saros are prominent examples of this type of feature (e.g. Şengör et al. 2005). The jog structures forming these basins directly control the geometric segment structure of the fault zone.

The NAF zone can be classified into three main parts—the Eastern, Central and Western (Figs. 1, 3). The Eastern and Central NAF are characterized by a narrow deformation zone, while the Western NAF presents a wide deformation zone.

The Eastern NAF extends for ~ 430 km between the Karlıova triple-junction and the Niksar releasing stepover. The Erzincan pull-apart basin is the most significant jog along this section. The 330 km-long western part of the section including the Ezinepazarı splay was ruptured during the Ms 7.9 1939 Erzincan earthquake. On the other hand, one of the present-day seismic gaps on the NAF zone exists the east of this section, along the Yedisu segment. The NAF to the west of Erzincan can be traced along a narrow zone through linear and distinct fault valleys in contrast to complex geometries through the Karlıova triple-junction area in the east.

The Central NAF is located between Niksar and Dokurcun. Starting at the north of the Niksar releasing stepover it extends as a ~ 525 km-long north vergent convex arc ending at the west end of the Dokurcun valley where the main strand splays into two branches. With the exception of segment boundaries, the central NAF is observed through a narrow deformation zone characterized by a regional scale restraining bend according to large bend geometry. The NAF has played an important role in the formation of the recent morphology of the region. It forms tectonic valleys and troughs outside the stepover areas. The Yeşilırmak and Kızılırmak rivers are deflected by the fault by ~ 17 and 25 km, respectively. The entire Central NAF was ruptured in the twentieth century by multi-segment events. These include the Ms 7.1 1942, Ms 7.4 1943, Ms 7.3 1944, Ms 7.1 1957 and Ms 7.2 1967 earthquakes.

To the west, the Western NAF bifurcates into two main strands namely the northern and southern strands. The northern strand is the main fault accommodating plate boundary motion through the Marmara Sea, Saros Bay and the North Aegean Trough (Barka and Kadinsky-Cade 1988; Barka 1992, 1996; Armijo et al. 1999, 2002, 2005; Şengör 1979a, b; Şengör et al. 1985, 2005; Le Pichon et al. 2001, 2003; Reilinger et al. 2006). The northern strand of the Western NAF extends for ~ 500 km between the Adapazarı Basin and the North Aegean Trough (Figs. 1, 3). Considering overall fault geometry, the western NAF is divided into two main geometric sections which are the Central Marmara arc (Le Pichon et al. 2001) and the north Aegean section from east to west. These two main sections are tied at the transpressional Ganos bend where fault orientation abruptly changes by $\sim 18^\circ$ (Armijo et al. 1999; Okay et al. 2004; Seeber et al. 2004). Both sections are highly segmented. Those segments are connected by releasing and restraining stepovers and bends. (Barka 1992, 1996; Armijo et al. 2002, 2005; Le Pichon et al. 2001, 2003; İmren et al. 2001; Ustaömer et al. 2008; Aksoy et al. 2010; Emre 2010; Emre et al. 2011a, b). The basins aligned along the strand in the Sea of Marmara, Gulf of Saros and North Aegean Trough are large scale morphotectonic structures developed in the releasing jogs, whereas submarine Central Marmara High (Le Pichon et al. 2001) and Ganos mountain represent uplifted relief in restraining bends. The southern strand of the Western NAF splays out from the main fault at Dokurcun valley and extends westward along İznik Lake and

Gemlik Bay where it connects with the NE–SW trending en echelon strike-slip fault systems around the Biga Peninsula (Barka and Kadinsky-Cade 1988; Barka 1992, 1996; Armijo et al. 1999; Şengör et al. 1985, 2005; Emre et al. 2010, 2011a, b, 2013). This strand is included in the Northwest Anatolia transition zone where recent crustal deformation is controlled by the bend kinematics (Emre et al. 2005a, b, c, 2011a, b; Özalp et al. 2013).

According to historical and instrumental earthquake records, the NAF is well-known as a source for several large earthquakes resulting in surface rupture. Figure 3 displays the distribution of surface ruptures developed by westward migration of the large earthquake sequence in the last century. Multi-segment faulting usually causing surface rupture have occurred in this sequence of earthquakes which started with the 1939 Erzincan earthquake in the east (Fig. 3). Many of these earthquakes have triggered a western fault segment as the next earthquake. Between the Erzincan basin and the Çınarcık basin in the Sea of Marmara Sea, ~900 km-of surface rupture has developed during these westward prograding earthquakes (Ambraseys 1970; Toksöz et al. 1979; Barka and Kadinsky-Cade 1988; Barka 1992, 1996, 1997; Stein et al. 1997a, b; Emre et al. 2003). These earthquakes from east to west are the 26th December 1939 Erzincan (Ms: 7.9), 20th December 1942 Erbaa–Niksar (Ms: 7.1), 26th November 1943 Tosya (Ms: 7.4), 1st February 1944 Bolu–Gerede (Ms: 7.3), 26th May 1957 Abant (Ms: 7.1), 22nd July 1967 Mudurnu Valley (Ms: 7.2), 13th March 1992 Erzincan (Mw: 6.3), 12th November 1999 Düzce (Mw: 7.2), 17th August 1999 İzmit (Mw: 7.4), respectively (McKenzie 1970; Ketin 1968; Ambraseys 1970; Dewey 1976; Barka and Kadinsky-Cade 1988; Stein et al. 1997a, b; Barka et al. 2000; Koçyigit 1988a, b, 1989, 1990; Tokay 1973; Pamir and Ketin 1941; Wright et al. 2000; Şengör et al. 2005).

In addition to them 32 medium-size earthquakes ($M > 5.0$) without surface rupture which can be related to the NAF zone have been recorded in the instrumental period (Kadirioğlu et al. 2016).

Within the historical period, 46 large earthquakes are estimated to have been generated from the NAF zone, with the majority of these earthquakes concentrated in the Marmara region (Ambraseys and Finkel 1995; Ambraseys 2002). Those data suggest that earthquake series occurred between 967 and 1050 along the Central NAF and in between 1719 and 1766 along the Western NAF. Those series appear to be analogous to the earthquake sequence of 1939–1999 (Ambraseys 1970, 2002; Ambraseys and Finkel 1987, 1995). The NAF has also produced very large earthquakes with up to 330–600 km-long surface ruptures like the 1509, 1668 and 1939 earthquakes (Ambraseys 1970; Ambraseys and Finkel 1995).

Especially, the noteworthy analyses of recent earthquake series reveal that the Marmara Sea portion of the NAF is prone to stress accumulation (Gürbüz et al. 2000; Parsons et al. 2000). Those studies suggest a 50% probability for a large earthquake along the NAF in the next 30 years' (Şengör et al. 2005; Parsons et al. 2000).

Geological and paleoseismological data indicate that the slip rate on the NAF over the past 10^3 – 10^5 year is ~15–22 mm/year (Hubert et al. 1997; Hubert-Ferrari et al. 2002; Okumura et al. 2003; Kondo et al. 2004; Kozacı et al. 2007, 2009, 2011; Pucci et al. 2007; Rockwell et al. 2009). On the other hand GPS studies suggest measured recent slip rates of 15–25 mm/year along the fault zone (Reilinger et al. 1997, 2006; Oral et al. 1995; Ayhan et al. 1995; McClusky et al. 2000, 2003; Meade et al. 2002). Recent studies propose GPS velocities along the NAF zone with a decelerating trend from east to west from 25 to ~17 mm/year (Reilinger et al. 2006; Tatar et al. 2012; Ergintav et al. 2014).

We divided the NAF zone into 38 geometric segments considering fault geometry and seismic behaviour. These are; Kargapazarı (1-1), Elmalı (1-2), Yedisu (1-3), Erzincan (1-

4), Refahiye (1-5), Suşehri (1-6), Reşadiye (1-7), Ezinepazar (1-8), Niksar (1-9), Erbaa (1-10), Destek (1-11), Havza (1-12), Köprübaşı (1-13), Kamil (1-14), Kargı (1-15), Ilgaz (1-16), Sarıalan (1-17), Bayramören (1-18), İsmetpaşa (1-19), Gerede (1-20), Yeniçağa (1-21), Bolu (1-22), Taşkesti (1-23), Dokurcun (1-24), Düzce (1-25), Karadere (1-26), Arifiye (1-27), Tepetarla (1-28), Gölcük (1-29), Karamürsel (1-30), Darıca (1-31), Adalar (1-32), Çınarcık (1-33), Avcılar (1-34), Kumburgaz (1-35), Tekirdağ (1-36), Ganos (1-37), Saros (1-38) segments (Fig. 3). However, detailed mapping of surface ruptures in twentieth century and paleoseismic data reveal that multi-segment rupturing is common on the NAF. Therefore we also present earthquake segments associated with large events in twentieth century (Table 1).

4.1.2 The East Anatolian fault

The East Anatolian Fault (EAF) (Arpat 1971; Arpat and Şaroğlu 1972, 1975; McKenzie 1972, 1978; Jackson and McKenzie 1984; Dewey et al. 1986; Taymaz et al. 1991a, b; Şaroğlu et al. 1992a, b; Westaway and Arger 1996; Westaway 2003, 2004; Duman and Emre 2013) constitutes a complex sinistral strike-slip fault zone that separates the Anatolian plate from the Arabian plate (Figs. 1, 3). The eastern part of the EAF exhibits a 295-km long narrow deformation zone where it takes the form of a single fault trace except for jog structures. However, to the west it is divided into northerly and southerly fault strands and becomes a 65-km wide deformation zone (Duman and Emre 2013). The southerly strand is the main fault. The main EAF zone is ~580 km-long between Karlıova and Antakya including the southern strand, and is divided into the 7 fault segments from NE to SW, namely, the Karlıova (2-1), Ilıca (2-2), Palu (2-3), Pütürge (2-4), Erkenek (2-5), Pazarcık (2-6), and Amanos (2-7) segments (Fig. 3). The lengths of the segments vary from 31 to 112 km, while their strikes vary from N35°E to N75°E. The northern strand of the EAF, called the Sürgü–Misis Fault (SMF) system, is ~380 km between Çelikhhan and the Gulf of İskenderun, exhibiting characteristic active left-lateral fault features (Duman and Emre 2013). It consists of 9 fault segments, which are, from NE to SW, the Sürgü (227), Göksun (226), Savrun (223), Çökak (222), Misis (216), Toprakkale (219), Yumurtalık (218), Karataş (217) and Düziçi–İskenderun (220) fault segments, respectively (Fig. 3).

The northern strand of the EAF connects to Misis–Kyrenia zone via the Gulf of İskenderun where the southern strand connects to the Dead Sea Fault (DSF) zone in the Karasu tectonic trough. Details of the jog structure in the Gulf of İskenderun are not known well. However, the EAF's connection to the DSF zone is provided by a large-scale extensional left-lateral stepover structure in the Karasu valley. Both transform faults overlap each other along this trough. Segments along the EAF do not display a significant order and they are bifurcated by either restraining or releasing bends or stepovers. The widths and lengths of the jogs vary from 1.5 to 25 km and from 6 to 45 km, respectively (Duman and Emre 2013).

Two surface ruptures that developed along the EAF in the twentieth century have been mapped. These are ruptures associated with the 1971 Ms 6.8 Bingöl earthquake (Fig. 3) and the 2010 Mw 6.1 Karakoçan earthquake (Arpat and Şaroğlu 1972; Seymen and Aydın 1972; Emre et al. 2010). Additionally it is known that the EAF to the east of Lake Hazar was also ruptured by the 1874 Ms 7.1, 1875 Ms 6.7, and 1866 Ms 7.2 earthquakes (Ambraseys 1988; Ambraseys and Jackson 1998; Çetin et al. 2003). Based on these observations Duman and Emre (2013) suggest that the next earthquakes maybe on segments farther west.

Table 1 Fault parameters for all 485 fault segments across Turkey

Segment	Fault			Length (km)	Trend (RHR)		Dip (Degree)		Slip rate (mm/year)		Depth (km)		Magnitude		References
	Type	ID No	AC		Min	Max	Min	Max	Min	Max	1	2	Obs.	Est. Mw	
Kargapazarı S	RL	1-1	H	39	77	120	87	90						6.94	
Elmalı S	RL	1-2	ER	27	273	302	87	90			16	24	1946 Ms 6.9	6.76	5;14;15; 19; 25; 27;31
Yedisu S	RL	1-3	H	77	279	311	87	90						7.27	
<i>1939 Earthquake segment</i>															
Erzincan S	RL	1-4		42					16						
Refahiye S	RL	1-5		49											14;15;
Suşehri S	RL	1-6	ER	330	65	264	319	87	90		18	20	1939 Ms 7.8	7.98	19;22;25;27;29; 31
Reşadiye S	RL	1-7		90											
Ezinepazar S	RL	1-8		76											
<i>1942 Earthquake segment</i>															
Niksar S	RL	1-9	ER	48	21	282	312	87	90		18	20	1942 Ms 7.1	7.04	15; 19; 28;29
Erbaa S	RL	1-10		15											
<i>1943 Earthquake segment</i>															
Destek S	RL	1-11		35											
Havza S	RL	1-12		35											
Köprübaşı S	RL	1-13		32											
Kamil S	RL	1-14	ER	280	35	250	355	87	90		18	20	1944 Ms 7.4	7.90	15;19;28;29
Kargı S	RL	1-15		57											
Ilgaz S	RL	1-16		39											
Saralan S	RL	1-17		22											
<i>1944 Earthquake segment</i>															
Bayramören S	RL	1-18		19						18	24				
İsmetpaşa S	RL	1-19		46											
Gerede S	RL	1-20	ER	180	31	250	277	90	90		18	19	1943 Ms 7.3	7.69	11;12; 15; 16; 19;28;29
Yeniçağa S	RL	1-21		37											
Bolu S	RL	1-22		37											
<i>1957 Earthquake segment</i>															
Taşkesti	RL	1-23	ER	40	254	272	85	90		18	15		1957 Ms 7.0	6.95	6;11;12;15;16;1 9
<i>1967 Earthquake segment</i>															
Dokurcun	RL	1-24	ER	70	267	323	85	90		18	15		1967 Ms 7.1	7.23	6;11;12; 15;16;19
<i>1999 Düzce Earthquake segment</i>															
Düzce S	RL	1-25	ER	40	258	307	85	90		18	15		1999 Mw 7.1	6.95	6;11;12; 15;16;19
<i>1999 İzmit Earthquake segment</i>															
Karadere S	RL	1-26		33,5											
Arifiye S	RL	1-27		31											
Tepetarla S	RL	1-28	ER	145	34	228	300	90	90		18	17	1999 Mw 7.4	7.58	11;12;13;15;16; 18;19;20
Gölcük S	RL	1-29		15											
Karamürsel S	RL	1-30		14											
Darca S	RL	1-31	H	15	265	290	87	90		18	15			6.48	11;12;15;16;19;
Adalar S	RL	1-32	H	44	92	131	55	85						7.00	20
Çınarcık S	NN-RL	1-33	H	35	264	295	55	85	22	27	13	15		6.90	20
Aveılar S	RL	1-34	H	30	64	107	65	85						6.81	11;12;15;16;19;
Kumburgaz S	RL	1-35	H	39	263	274	85	90		18	17			6.94	20
<i>1912 Earthquake segment</i>															
Tekirdağ S	RL	1-36	ER	140	35	263	275	80	90		18	19		6.89	
Ganos S	RL	1-37		90	247	263	75	90		18	20		Ms 7.4	7.35	11;12;15;16;19; 20
Saros S	RL	1-38	H	42	74	93	42	45		18	20			6.98	
<i>East Anatolian FZ</i>															
Karlıova S	LL	2-1	H	31	210	255	90	90		8	8			6.83	
İlica S	LL	2-2	ER	37	210	229	90	90		18	20		1971 Ms 6.8	6.92	5.7.9.15.19.25.2 7.31
Palu S	LL	2-3	H	77	218	248	85	90		9	10			7.27	
Gökdere jog	LL	2-3-1	H	14	232	278	85	90		18	18			6.44	

Table 1 continued

Fault		Length (km)	Trend (RHR)	Dip (Degree)	Slip rate (mm/year)		Depth (km)		Magnitude		References		
Segment	Type				ID No	AC	Min	Max	1	2		Obs.	Est. Mw
Pütürge S	LL	2-3-2	H	24	230	288	85	90			6.71		
	LL	2-3-3	H	24	198	292	85	90			6.71		
	LL	2-4	H	97	230	249	85	90			7.39		
	LL	2-5	H	77	233	268	85	90			7.27		
	LL	2-6	H	82	16	254	85	90	6	7	7.30		
	LL	2-7	H	114	10	44	85	90	4	5	7.46		
	NN	3	H	21	156	199	65	60			6.61		
	RL	4	H	46	229	257	87	90			7.02		
												20	
Edremit FZ													
Küçükkuyu S	NN	5-1	H	23	73	85	50	65			6.66		
	NN	5-2	ER	90	28	52	111	50	18	16	1944 Ms 6.8	6.77	
	NN	5-3	H	16	15	47	50	65	18	15		6.45	
Çan S	RL	6-1	H	20	229	252	87	90			6.62		
	RL	6-2	H	42	14	191	231	87	13	15	6.44		
	RL	6-3	H	15	239	243	87	90			6.48		
Sarıköy F	RL	7	H	66	229	288	87	90			7.20		
	RL+R	8	H	26	219	279	35	50	18	16	6.74		
	RL	9	H	45	243	283	87	90			7.01		
	RL	10	H	32	264	274	85	90	13	15	6.85		
	RL	11	H	36	260	281	87	90			6.90		
	RL-R	12	H	44	238	281	70	90	18	16	7.00		
	RL	13	H	38	269	304	85	90			6.93		
	RL	14	H	23	266	280	85	90			6.69		
	RL	15	Q	18	221	249	87	90			6.57		
	RL	16	ER	70	87	305	85	90	13	15	1953 Ms 7.3	7.30	
Manyas FZ	NN+	17-2	ER	40	16	277	311	80	13	15	1964 Ms 6.8	6.51	
	RL	17-1		16							6.51		
	RL	19	H	19	219	247	85	90			6.59		
	RL	20	H	34	217	259	87	90	13	15	6.88		
	NN	21	Q	9	311	311	45	60			6.12		
	NN	22	Q	14	185	198	65	70			6.37		
Havran S	RL	23-1	H	19	241	271	87	90			6.59		
	RL	23-2	H	90	28	234	263	87	18	16	6.78		
	RL	23-3	H	16	236	266	87	90			6.51		
	RL+R	23-4	H	21	257	296	87	90			6.64		
Gökçeyazı S	RL	24-1	H	65	39	253	270	87	18	16	6.94		
	RL+N	24-2	H	25	265	308	87	90			6.73		
	RL	25	Q	18	204	218	87	90	13	13	6.52		
	NN	26	H	9	248	265	65	70			6.12		
Soma-Kırkağaç FZ	NN	27-1	H	17	222	267	65	70			6.48		
	NN	27-2	H	20	298	358	65	70	13	14	6.58		
	NN	27-3	H	27	0	359	65	70			6.90		
East S	RL	28-1	H	35	3	50	87	90	18	16	6.89		
	RL	28-2	H	36	6	40	87	90			6.90		
	RL+N	29-1	Q	13	90	121	85	90			6.41		
	RL+N	29-2	Q	9	90	115	85	90	18	16	6.23		
Düvertepe FZ	RL+N	29-3	Q	16	112	136	85	90			6.51		
	RL	30-1	H	35	267	306	87	90			6.89		
	RL	30-2	H	54	277	308	87	90			7.10		
Çaysimav S	RL	30-3	H	23	286	312	87	90			6.69		
	RL	30-4	H	205	33	287	308	87	3,4	3,4	18	16	6.86
	RL	30-5	H	24	3	359	87	90			6.71		
	RL	30-6	H	27	270	298	87	90			6.76		
	RL	30-7	H	18	303	323	87	90			6.57		
	NN	31-2	Q	15	147	172	87	90	13	13	6.41		
NN	31-1	Q	14	172	196	87	90			6.37			

Table 1 continued

Fault				Length (km)	Trend (RHR)		Dip (Degree)		Slip rate (mm/year)		Depth (km)		Magnitude		References	
Segment	Type	ID No	AC		Min	Max	Min	Max	Min	Max	1	2	Obs.	Est. Mw		
Mordoğan F	NN	32	Q	12	11	11	65	70						6.28		
Gülbahçe FZ	RL	33-1	H	21	4	14	87	90						6.64	21;23	
	RL	33-2	H	24	3	12	87	90		13				6.71		
	RL	33-3	H	24	338	351	87	90		13				6.71	3; 19; 24	
Yağcılar F	RL	34	ER	12	3	359	87	90				2005 Mw 5.9	6.37	21;23		
Seferhisar F	RL	35	H	25	203	225	87	90		13	13		6.73	23; 30		
Güzelhisar F	RL	36	Q	24	285	302	0	90					6.68	23		
Menemen FZ	NN	37	H	11	128	128	65	70					6.23	23		
İzmir F	NN	38-1	H	19	250	281	65	70		13	13		6.55	23; 30		
	NN	38-2	H	19	245	283	65	70					6.59	23		
Tuzla F	RL	39-2	H	16	11	54	87	90					6.51	23		
Tuzla F	RL	39-1	H	24	34	59	87	90					6.68	23; 30		
Gümmüdürlü F	NN	40	H	14	86	155	55	65					6.44			
Dagkızılca F	RL	41	H	27	216	239	87	90		13	13		6.75	23		
Unnamed F	NN	42	Q	7	296	296	87	90					5.98			
Unnamed F	NN	43	Q	6	292	292	87	90					7.20			
Gediz GS	Alaşehir S	NN	44-1	ER	45	285	345	65	70			1969 Ms 6.5	7.04	4;23		
	Salihli S	NN	44-2	H	30	254	307	65	70				6.81			
	Akçapınar S	NN	44-3	H	14	254	300	55	70				6.37			
	Armutlu S	NN	44-4	H	35	51	102	55	70				6.90			
	Nifdağı S	NN	44-5	H	11	247	264	65	70				6.23	23		
	Kemalpaşa F	NN	44-6	H	24	267	313	55	70				6.68			
	Manisa F	NN	44-7-2	H	26	272	333	55	65				6.73			
		NN	44-7-1	H	35	1	358	55	65				6.90			
	Killik F	NN	44-8	H	50	102	147	60	70		13	14		7.10	4;23	
	Çapaklı S	NN	44-9	H	11	69	124	65	70				6.23			
	Kemerdağları S	NN	44-10	H	18	112	175	65	70				6.52			
	Halitpaşa F	NN	44-12	H	23	279	325	65	70				6.66			
	Ozanca F	NN	44-13	H	27	295	360	65	70				6.75			
		NN	44-13-1	H	11	106	162	65	70				6.23			
	Gölmarmara F	NN	44-14	H	18	301	335	65	70				6.52			
	Akselendi F	NN	44-15	H	19	90	221	65	70				6.55			
	Akhisar F	NN	44-16	H	12	297	322	65	70				6.37	23		
Muradiye F	LL	44-17	H	8	28	97	87	90				6.50				
Unnamed F	LL	45	Q	15	13	54	87	90				6.48				
Unnamed FZ	LL	46	Q	10	54	70	87	90				6.28				
Unnamed F	RL	47	Q	9	24	43	87	90				6.23				
Köprübaşı FZ	RL	48	H	23	215	237	87	90		13	14		6.66	4;23		
Kiraz F	R	49	Q	13	115	126	70	80				6.33				
Efes F	NN	50	H	8	5	360	64	65				6.05				
Kuşadası FZ	NN	51	H	18	58	89	50	70				6.52				
Davutlar F	NN	52	Q	8	253	280	65	70				6.60				
Büyük Menderes GS	Söke F	NN+	53-1-1	H	22	30	76	55	66				6.63	23		
		RL														
	İncirliova S	NN+	53-1-2	H	13	25	63	55	66				6.33			
		RL														
	Umurlu S	NN	53-2	H	31	83	133	55	60		13	14		6.83		
	Atça S	NN	53-3	H	25	54	104	50	65				6.71			
Pamukören S	NN	53-4	H	34	62	122	50	65				6.88				
Buharkent S	NN	53-5	H	26	70	98	50	65				6.73	4;23			
Milas F	Çine F	NN	54	Q	22	298	319	60	70		13	14		6.63	23	
		NN	55	Q	30	1	360	63	60				6.81	4;23		
	Unnamed F	NN	56	Q	7	63	74	87	90		13	13		5.98	23	
	Unnamed F	NN	57	Q	9	235	252	87	90				6.70			
Beçin S	RL	58-1	H	25	292	309	87	90		13	14		6.73			
	RL	58-2	H	14	295	307	87	90					6.50			
Yatağan F	NN	59	H	17	297	342	60	65					6.48	23		
	NN	60	H	25	105	140	60	65					6.71			
	NN	61-1	Q	16	114	160	55	60		13	14		6.45			
	NN	61	Q	10	91	119	55	60					6.18			

Table 1 continued

Segment	Fault			Length (km)	Trend (RHR)		Dip (Degree)		Slip rate (mm/year)		Depth (km)		Magnitude		References	
	Type	ID No	AC		Min	Max	Min	Max	Min	Max	1	2	Obs.	Est. Mw		
Gökova FZ	NN	62-1	H	>60	9	60	80	55	65	13	14				6.12	
	NN	62-2	H		21	75	85	55	65						6.61	
	NN	62-3	H		9	85	95	55	65						6.12	
	NN	62-4	H		22	75	100	55	65						6.20	
Datça F	NN	63	Q	10	107	114	50	65							6.18	
Selimiye F	NN	64	Q	21	244	284	60	65							6.61	
Bozburun F	NN	65	Q	11	250	282	60	65		13	14				6.23	
Taşlıca F	NN	66	Q	11	43	63	60	65	6.23							
Kekova F	NN	67	H	18	221	260	65	70	6.52							
Kale F	NN	68	H	32	43	93	55	65	6.50							
Eşen F	NN+	69-1	Q	18	118	161	60	65		13	14				6.52	
	NN+	69-2	Q	24	175	216	60	65	6.68							
	NN+	69-3	Q	12	166	227	60	65	5.80							
Unnamed F	NN	70	Q	5	9	18	60	65							5.94	
Unnamed F	LL	71	H	13	196	209	87	90							6.41	
Altınyayla F	LL	72	H	18	182	221	87	90							6.52	
Acıpayam F	NN+	73-1	Q	20	33	46	87	90							6.58	
	LL															
	NN+	73	Q	24	14	52	87	90							6.68	
Keleçi F	NN	74	Q	28	208	240	65	70		13	14				6.78	
Çameli F	LL	75	H	29	199	234	87	90	6.79							
Beyağaç F	NN	76	H	14	113	145	60	70	6.37							
Göktepe F	NN	76-1	H	6	66	118	60	70							5.89	
	NN	77	Q	19	1	358	60	70							6.55	
Karacasu F	NN	78	Q	26	1	359	60	71							6.73	
Unnamed F	NN	79	Q	13	280	330	60	65							6.41	
Tekkeköy F	RL+N	80	H	11	311	325	87	90							6.23	
Cankurtaran F	NN	81	Q	11	148	168	55	65							6.60	
Denizli GS	Pamukkale FZ	NN	82-1-1	Q	7	310	330	60	65						5.98	
		NN	82-1-2	H	12	305	315	60	65						6.28	
		NN	82-1-3	H	12	265	325	60	65						6.28	
		NN	82-1-4	H	11	310	330	60	65						6.23	
		NN	82-1-5	H	9	290	305	60	65						6.12	
	Buldan FZ	NN	82-2	H	11	260	300	60	65						6.23	
	Sarayköy FZ	NN	82-3	H	18	293	312	55	70						6.52	
	Denizli FZ	NN	82-4	H	24	274	336	55	70		13	14				6.68
	Babadağ FZ	NN	82-5	Q	19	279	328	55	70	6.55						
		NN	82-5-1	Q	11	291	328	55	70	6.23						
		NN	82-6-2	H	8	208	246	55	65	6.05						
	Honaz F	NN	82-6-1	H	10	273	295	55	65						6.18	
	Kaklık F	NN	82-6-3	H	7	273	301	55	65							5.98
		NN	82-7	H	9	114	127	55	65							6.12
Unnamed F	NN	83	Q	12	239	250	60	65							5.90	
Unnamed F	NN	84	Q	6	0	358	65	70		13	14				6.50	
Acıgözü GS	NN	85-1-1	H	13	42	50	65	75								
	NN	85-1-2	H	17	95	110	65	75							6.48	
	NN	85-2-1	H	10	35	55	65	75		13	14				6.18	
	NN	85-2-2	H	11	55	90	65	75	6.23							
	NN	85-2-3	H	22	229	286	65	75	6.63							
	NN	85-2-4	Q	11	229	286	65	75	6.23							
	NN	85-2-5	Q	16	259	331	65	75	6.45							
NN	85-2-6	Q	22	259	331	65	75	6.63								
Burdur GS	Karakent F	NN	86-1	H	33	18	49	65	75							
	Hacılar S	NN	86-2	ER	32	190	264	45	60		13	14	1914 Ms 7.0		6.85	
	Gökçebağ S	NN	86-3	H	30	203	278	45	60	6.60						
Davras FZ	NN	87-1	H	21	201	254	60	65		13	15				6.61	
	NN	87-2	Q	10	211	249	60	65	6.28							
	RL	88	H	32	0	360	87	90	6.85							

Table 1 continued

Fault				Length (km)	Trend (RHR)		Dip (Degree)		Slip rate (mm/year)		Depth (km)		Magnitude		References
Segment	Type	ID No	AC		Min	Max	Min	Max	Min	Max	1	2	Obs.	Est. Mw	
Barla F	NN	89	H	14	10	41	65	70						6.37	
Mahmatlar F	NN	90	H	14	161	265	70	75						6.37	
Sarıdris F	NN	91	H	14	144	171	65	75						6.37	
Beyşehir Gölü F	NN+ RL	92	Q	32	315	353	87	90						6.85	
Gelendost F	NN	93	H	25	208	313	55	70						6.71	
Kumdanlı F	NN+ LL	94	H	16	214	255	65	80						6.45	
	NN	94-1	Q	16	190	254	65	70						6.45	
Senirkent FZ	NN	95	Q	20	224	296	65	70						6.58	
Uluborlu F	NN	96	H	11	239	267	60	65						6.23	
Yarıkkaya F	NN	97	Q	11	236	259	65	70						6.23	10;23
Unnamed F	NN	98	Q	10	194	254	87	90						6.18	
Koçbeyli F	NN	99	H	13	189	252	70	70						6.33	
Arızlı F	NN	100	H	15	193	256	60	60						6.41	23
Karaadilli F	NN	101	H	14	163	269	55	65						6.37	
Tatarlı F	NN	102	H	24	212	267	65	70						6.70	
Unnamed FZ	NN	103	Q	10	211	290	87	90						6.18	10;23
Çivril-Dinar GS	Dinar F	NN	104-1	H	28	108	231	45	80					6.77	
		NN	104-2-1	H	12	315	330	45	70					6.28	
	Baklan F	NN	104-2-2	ER	55	12	109	231	45	75			1995 Mw 6.4	6.28	
		NN	104-3	H	16	310	355	45	75		13	14		6.45	23
	Çivril F	NN	105-1	H	11	208	228	55	70					6.23	
		NN	105-2	H	14	207	262	55	70					6.37	
		NN	105-3	H	8	260	314	55	70					6.05	
		NN	106-1	H	38	24	30	85	40	75				6.70	
		NN	106-2	H	20	11	105	40	75					6.58	
	Sivaslı F	NN	107	Q	24	154	210	55	65					6.71	
Kızılören F	NN	108	Q	15	201	240	87	90					6.41		
Düzbel F	LL	109	Q	13	43	68	87	90					6.33		
Örenkaya F	NN	110	Q	29	5	48	87	90					6.79		
Sandıklı F	NN	111	Q	11	204	223	87	90					6.23		
Akharım F	NN	112	Q	14	6	64	70	75					6.44		
Unnamed F	NN	113	Q	11	303	317	65	68					6.23	23	
Unnamed F	LL	114	Q	9	217	224	87	90		13	14		6.12		
Unnamed F	NN	115	Q	5	25	25	87	90					5.94		
Güre FZ	NN	116	Q	21	266	324	70	75					6.61		
Selendi F	RL+N	117	H	16	4	67	75	80					6.45		
Rahmanlar F	NN+ RL	118	Q	22	57	61	65	80					6.60		
Kızılızüüm F	NN	119	Q	10	42	42	65	70					6.18		
Emet Gediz FZ	Emet S	NN	120-1	Q	22	1	360	55	65					6.63	
		NN	120-3	Q	23	138	174	87	90					6.69	
	Gediz S	NN	120-2	ER	38	8	356	55	65		18	16	1971 Ms 7.1	6.93	
		RL	121	H	29	97	129	87	90					6.79	23
	Çukurören F	RL	121-1	H	18	108	126	87	90					6.52	
		NN	122	H	15	98	174	60	65					6.48	
	Ashıhanlar F	NN	123	Q	6	96	177	87	90		18	15		5.89	
	Çatkuyu F	LL	124	H	10	317	334	87	90					7.00	
	Gecek F	NN	125	H	10	85	94	70	70		13	15		6.18	
	Afyon-Alşehir GS	Sultandagi F	NN	126-1-1	Q	100	18	309	330	55	70			2002 Mw 6.5	6.52
ER			11	241	309	50	70						6.23		
NN		126-1-3	H	22	305	330	55	70					6.63		
NN		126-1-4	H	26	303	325	55	70					6.73		
NN		126-1-5	H	20	309	327	55	70					6.58		
NN		126-1-6	H	18	312	329	55	70					6.52		
Gazlıgöl F		NN	126-2	H	19	1	358	60	65		13	15		6.55	10;23
		NN	126-3	H	8	0	358	60	70					6.05	
Erkmen F		NN	126-4-1	H	12	249	318	55	65					6.28	
		NN	126-4-2	H	16	238	303	55	65					6.45	
İsıklar FZ	NN	126-5-1	H	16	267	300	85	90					6.45		
	NN	126-5-2-1	H	12	16	54	85	90					6.28		
Kali Çayı FZ	NN	126-5-2-2	H	13	21	111	85	90					6.33		

Table 1 continued

Fault				Length (km)	Trend (RHR)		Dip (Degree)		Slip rate (mm/year)		Depth (km)		Magnitude		References
Segment	Type	ID No	AC		Min	Max	Min	Max	Min	Max	1	2	Obs.	Est. Mw	
Çobanlar FZ	NN	126-5-3	H	19	165	275	85	90						6.55	
	NN	126-6-1	H	23	88	116	55	65						6.66	
	NN	126-6-2	H	21	5	353	55	65						6.61	
Bolvadin F	NN	126-7	H	7	54	54	65	75						5.98	
Büyük Karabağ F	NN	126-8	H	29	28	54	65	75						6.79	
	NN	126-9	H	23	205	227	60	65						6.66	
Çukurecek F	NN	126-10-1	H	18	0	359	55	75						6.52	
	NN	126-10-2	H	9	278	300	55	75						6.12	
Yunak Fz	NN	126-10-3	H	27	34	83	55	75						6.75	
	NN	126-10-4	H	20	165	195	55	75						6.58	
Piribeyli F	NN	126-11	H	17	89	200	60	65						6.48	
Yavaşlı F	NN	126-12	H	22	182	200	70	70						6.63	
İlgın FZ	NN	126-13-1	H	27	1	357	65	67						6.76	
	NN	126-13-2	H	9	194	242	65	67						6.60	
Yazlıca F	RL	126-14	H	20	233	327	87	90						6.58	
Naşa FZ	NN	127	H	21	104	158	55	65		13	14			6.61	
	NN	127-1	H	9	156	166	55	65						6.12	
Çavdarhisar F	NN	128	Q	12	137	158	65	70						6.28	
Tavşanlı F	NN	129	H	15	261	300	70	80						6.41	
Şahmelek F	NN	130	H	15	250	311	70	80						6.41	
Kütahya F	NN	131	H	48	284	306	60	75						7.04	
Parmakören F	NN	132	H	14	91	121	60	75						6.44	
Seyitömer F	RL	133	Q	13	302	314	87	90						6.33	
Orhaneli F	RL	134	H	29	291	320	87	90		18	16			6.79	
Soğukpınar F	NN+	135	H	22	104	159	75	80						6.63	
	RL	135	H	22	104	159	75	80						6.63	
Bursa F	NN	136	H	35	260	320	55	70						6.90	
İnegöl FZ	NN	137-1	H	21	105	127	55	65						6.61	
	NN	137-2	H	12	45	149	55	65						6.28	
Oylat F	NN	138-1	H	20	0	354	70	75						6.62	
	NN	138-2	H	17	280	311	70	75						6.54	
Dodurga F	NN	139-1	H	19	290	310	85	90		18	16			6.59	
	NN	139-2	H	16	285	324	85	90						6.45	23
Eskişehir F	NN-RL	140-1	H	16	289	309	70	85						6.45	
	NN+	140-2	H	19	286	311	70	85		18	16			6.55	
	RL	140-3	H	20	270	311	70	85						6.70	
	NN+	140-4	H	20	280	307	70	85						6.62	
Kaymaz F	RL	141	Q	26	293	298	85	90						6.73	
Unnamed F	NN+	142	Q	9	303	306	85	90						6.23	
Unnamed F	NN+	143	Q	10	307	319	85	90		18	16			6.18	
Taycılar F	LL	144	Q	20	53	90	85	90						6.62	
Barakfakı F	NN	145	H	10	285	310	65	70						6.28	13;18
Gençali F	RL	146	H	23	247	271	85	90						6.69	
Gemlik F	RL	147	H	25	270	307	85	90						6.73	20
İznik Mekece F	RL	148	H	44	256	271	85	90		18	17			7.03	
	RL	149	H	62	246	275	85	90						7.23	13;18
Geyve F	NN	150	Q	6	246	259	80	85		18	15			6.03	20
Armutlu F	NN	151	Q	14	267	291	70	75						6.37	13;20
Esenköy F	NN	152	H	29	295	316	87	90						6.78	
Orhangazi F	RL+N	153	H	20	258	303	65	75						6.62	
Yalova F	NN	153	H	20	258	303	65	75						6.62	13;18;20
Altınova F	R	154	H	9	240	275	55	65						6.23	
Yalakdere F	RL	155	H	25	242	259	87	90		13	15			6.71	
Hendek F	RL	156	H	36	226	272	87	90						6.90	18
Çilimli F	R	157	H	30	217	264	35	40						6.80	
	R	157-1	H	17	234	264	35	40		18	17			6.54	
Yığılca F	R	158	Q	42	231	273	40	60						6.98	6
Devrek F	RL	159	Q	29	202	238	60	75						6.79	

Table 1 continued

Fault				Length (km)	Trend (RHR) Min Max	Dip (Degree) Min Max	Slip rate (mm/year)		Depth (km)		Magnitude		References	
Segment	Type	ID No	AC				Min	Max	1	2	Obs.	Est. Mw		
Karabük F	R	160	Q	29	214	214	60	75				6.80		
Kurumcu F	NN	161	Q	7	279	279	65	70				5.98		
Orta F	LL	162	H-ER	28	186	226	87	90			2000 Mw 6.1	6.78	29	
Çamlidere F	NN	163	H	16	265	294	65	67				6.45		
Cihanbeyli F	RL	164	H	56	99	135	87	90				7.17		
Altıntekin F	NN	165	Q	29	145	225	60	62				6.79		
Unnamed F	NN	166	Q	9	54	54	87	90	13	15		6.12	23	
Konya F	NN	167	H	17	18	30	75	80				6.48		
Alacadağ FZ	NN	168	Q	19	178	215	80	85				6.55		
Hotamış F	NN	169	H	16	172	214	67	75				6.45		
Berendi F	NN	170	Q	13	76	127	80	85				6.33		
Akhöyük EF	NN	171	H	2	334	334	80	85				5.26		
Nasuhpınar F	NN	172	H	14	202	226	70	80				6.37	29	
Seyithacı F	NN	173	H	20	2	358	65	75				6.80		
Leskeri FZ	NN	174	Q	22	8	32	80	85	13	18		6.63		
Tuzgözü FZ	Bor S	NN	175-1	H	30	113	164	67	75			6.81		
	Altunhisar S	NN	175-2	H	20	146	163	65	75			6.58		
	Helvadere S	NN+ RL	175-3	H	200	40	134	154	65	80	13	18	6.97	29
	Açıpınar S	NN	175-4	H	58	131	159	65	70			7.19		
	Koçhisar S	NN	175-5	H	41	86	185	60	70			6.30		
	Büyükkısla S	NN	175-6	H	11	105	196	65	75			6.23		
Merzifon Esençay FZ	Ovalıbağ S	NN	176	Q	13	180	195	80	85			6.33		
	Derinkuyu F	NN	177	Q	19	164	185	75	80			6.55		
	Unnamed FZ	NN	178	Q	18	138	196	80	85	13	15	6.52	29	
	Unnamed F	NN	179	Q	5	337	348	80	85			5.94		
	Gümüşkent F	NN	180	Q	35	74	139	65	70			6.89		
	Akpınar F	RL	181	ER	33	307	326	87	90	18	16	1938 Ms 6.8	6.86	
	Bala F	RL	182	H	14	145	151	87	90	13	18		6.44	
	Karakeçili FZ	LL-R	183	H	36	187	239	70	75	18	16		6.90	29
	Keskin FZ	RL	184	Q	13	170	189	87	90	13	16		6.36	
	Çankırı F	R R	185-2 185-1	Q Q	73	35 38	161 181	200 217	40 55	18	16		7.20 6.93	
Merzifon Esençay FZ	Esençay S	RL	186-1	H	61	276	306	85	90			7.16		
	Amasya S	RL	186-2	H	34	266	319	85	90	13	15	6.88		
	Sultuova S	RL	186-3	H	34	265	288	85	90			6.88		
	Dıphacı S	RL	186-4	H	227	38	244	290	85	90		6.93	29	
	Laçın S	RL	186-5	H	31	265	297	85	90			6.30		
	İskilip S	RL	186-6	H	31	265	274	85	90	18	16	6.82		
	Unnamed F	R	187	Q	12	201	259	55	60	13	15		6.37	
	Sungurlu F	RL RL	188-1 188-2	Q Q	122	82 35	217 224	261 255	87 90	18	15		7.30 6.89	
	Unnamed F	RL	189	Q	10	228	254	87	90	18	16		6.28	
	Turhal F	RL	190	H	26	258	292	87	90				6.74	
	Almus F	RL	191	H	59	263	299	87	90				7.14	
	Gökçe F	RL+R	192	H	19	244	256	60	80				6.59	
	Kazankaya F	RL	193	Q	46	231	251	87	90				7.02	29
	Çekerek F	RL	194	H	43	241	263	87	90				7.02	
	Buğdaylı F	RL	195	H	24	263	264	87	90	13	15		6.71	
Unnamed F	NN	196	Q	6	216	216	87	90				5.89		
Akmağdeni F	LL	197	H	35	232	241	87	90				6.89		
Boğazlıyan F	NN	198	Q	11	299	299	87	90				6.33		
Yemliha F	LL	199	Q	16	242	263	87	90				6.47		
Yuvahı F	LL	200	Q	22	210	268	87	90				6.66		
Divriği F	R	201	H	69	231	326	40	50	18	20		6.70	25;29	
Central Anatolian FS	Deliler F													
	Bünyan S	LL	202-1	H	204	26	227	241	87	90		6.74		
	Sarıoğlan S	LL	202-2	H	37	233	270	87	90	18	20	6.92	29	
	Dökmetaş S	LL	202-3	H	44	230	253	87	90			6.70		
	Tecer S	LL	202-4	H	92	229	279	87	90			7.45		
	Erkilet FZ	NN+ LL	203-1	H	23	38	85	87	90	0.8	1.0		6.69	
Central Anatolian FS	Erkilet FZ	NN+	203-2	H	24	6	73	87	90	18	20		6.71	29
		LL	204-1	H	56	30	206	216	87	90			6.81	

Table 1 continued

Fault				Length (km)	Trend (RHR)		Dip (Degree)		Slip rate (mm/year)		Depth (km)		Magnitude		References		
Segment	Type	ID No	AC		Min	Max	Min	Max	Min	Max	1	2	Obs.	Est. Mw			
İncesu FZ	LL+N	204-2	H	25	197	216	87	90						6.71			
		NN	205	Q	23	0	360	80	85						6.66		
	Yeşilhisar FZ	NN+	206-1	H	10	3	359	80	85						6.18		
			LL	206-2	H	18	8	357	80	85					7.10		
		NN+	206-3	H	12	327	359	80	85					6.37			
	Ecemiş F	LL	207-1	H	54	188	207	85	90						6.20		
			LL	207-2	H	109	61	188	223	85	90	18	20			7.22	29
	Çamlıyayla F	NN	208	Q	11	49	81	50	55						6.33		
			Aladağ F	NN	209	Q	36	25	70	80	85	18	20			7.30	9
			Unnamed F	LL	210	Q	17	53	82	87	90					6.54	
Sarız F	Bakırdağ S	LL	211-1	H	87	217	283	87	90						7.33		
		LL	211-2	H	215	26	207	255	87	90	18	20			6.74	9	
		LL	211-3	H	56	204	242	87	90					6.80			
		LL	211-4	H	46	230	255	87	90					7.02			
	Demirooluk F	LL	212	H	28	192	228	87	90						6.78	9	
			Çatalcam F	LL	213	H	17	208	217	87	90	18	20			6.54	
			Saimbeyli F	LL	214	H	41	201	225	87	90					6.97	1;9
			Unnamed F	LL	215	Q	27	152	211	87	90					6.76	9
			Misis F	LL	216	H	34	1	360	85	90					6.88	
			Karataş F	LL	217	H	63	213	243	85	90	18	35			6.60	1;9
Yumurtaalık F	LL	218	H	41	213	247	85	90						6.97			
		Toprakkale F	LL	219-1	H	20	137	243	85	90	18	35			6.62	9	
				219-2	H	35	164	247	85	90					6.50		
219-3	H			49	200	237	85	90					7.09	1;			
Düzici-İskenderun FZ	NN	220-1	H	19	146	212	70	80						6.55			
		Osmaniye S	NN	220-2	H	24	208	268	70	80	18	15			6.68	2	
		Erzin S	NN	220-3	H	9	151	206	70	80					6.70		
		Payas S	NN	220-4	H	21	187	199	70	80					6.64		
Çokak F	LL	221	H	24	178	222	87	90						6.71			
		Unnamed F	LL	222	H	13	208	208	87	90	18	20			6.30	9	
		Savrun F	LL	223	H	60	207	236	87	90					7.17		
Kahramanmaraş FZ	R	224-1	H	12	258	291	40	50						6.32			
		R	224-2	H	15	247	298	40	50	18	15			6.70	9		
		R	224-3	H	15	230	281	40	50					6.43			
Engizek FZ	R	225-1	Q	23	244	280	40	50						6.66			
		R	225-2	Q	16	266	322	40	50	18	15			7.30	9		
		R	225-3	Q	14	235	273	40	50					6.44			
Çardak F	LL	226	H	85	201	292	87	90						7.32	5		
		Sürgü F	LL	227-1	H	55	228	277	87	90	18	20			6.90		
Malatya F	LL	227-2	H	24	248	305	87	90						6.71			
		Beyyurdu F	LL	228	H	37	248	283	87	90					6.92	25;5	
		Gürün F	LL	229	H	31	231	258	87	90	18	18			6.83		
		Ayvalı F	RL	230	H	22	111	129	87	90					6.66		
		Doğanshehir FZ	LL	231	H	29	195	244	87	90					6.80		
		Akçadağ S	LL	232-1	H	74	201	231	87	90					7.25	5;25	
Munzur S	LL	232-2	H	37	182	215	87	90	18	20				7.10			
		Kemaliye S	LL	232-3	H	65	153	210	87	90					7.19	25;31	
		Ovacık F	LL	233-1	H	50	218	264	87	90					6.50	25;31	
Munzur S	LL			233-2	H	86	234	261	87	90	18	20			7.33	14;25;31	
Heltepe F	LL	234	H	15	22	50	87	90	18	15				6.48	14;25;31		
		Pülümür F	RL	235	H	28	257	308	87	90	18	18			6.70		

Table 1 continued

Segment	Fault				Length (km)	Trend (RHR)		Dip (Degree)		Slip rate (mm/year)		Depth (km)		Magnitude		References
	Type	ID No	AC			Min	Max	Min	Max	Min	Max	1	2	Obs.	Est. Mw	
Nazimiye F	RL	236	H		51	279	300	87	90			18	20		7.07	
Karakoçan FZ	RL	237	H		25	277	295	87	90			18	18		6.10	
	RL	237-1	H		17	305	308	87	90						6.54	
Unnamed F	RL	238	H		7	304	304	87	90			18	15		6.11	
Sancak-Uzunpazar FZ	LL	239	H		51	33	104	87	90			18	20		7.07	
Sudüğünü F	RL	240	H		24	256	329	87	90			18	18		6.71	5;25;31
Sudüğünü F	LL	240-1	H		16	127	144	87	90						6.51	
Unnamed F	LL	241	H		13	34	52	87	90						6.41	
Unnamed F	RL	242	H		7	337	343	87	90						6.11	
Unnamed F	LL	243-1	H		7	32	52	87	90						6.11	
Unnamed F	LL	243	H		5	332	333	87	90			18	15		5.94	
Unnamed F	LL	244	H		12	176	235	87	90							
Unnamed F	LL	245	H		8	52	52	87	90						6.05	
Unnamed F	LL	245-1	H		5	326	326	87	90						5.78	
Bahçeköy FZ	NN+	246	H		27	2	360	87	90			18	18		6.76	
	LL															
Unnamed FZ	NN+	248	H		5	84	91	87	90			18	15		5.94	
Tercan F	RL	249	H		36	271	293	87	90						6.90	
Unnamed F	RL	250	H		7	283	309	87	90						6.11	
Unnamed F	RL	251	H		7	288	288	87	90						6.11	25;31
Unnamed F	RL	252	H		8	274	298	87	90			25	25		6.17	
Unnamed F	LL	253	H		9	33	68	87	90							
Kandilli F	RL	254	H		28	272	308	87	90						6.78	
Çat FZ	LL	255	Q		19	40	53	87	90						7.00	
Palandöken F	LL+R	256	H		54	49	77	87	90						7.10	
Erzurum FZ	Nenehatun S	LL	257-1	H		41	10	40	87	90					6.97	
	Dumlu S	LL	257-2	H		39	0	357	87	90		25	25		6.90	25;31
	Böreklı S	LL+R	257-3	H		12	29	58	87	90					6.32	
Pasinler FZ	R	258	H		35	35	133	45	60			25	25		6.70	25;31
Karayazi F	RL	259	H		59	70	129	87	90						7.14	
Horasan Senkaya FZ	Gerek S	LL+R	260-1	ER		25	192	229	87	90				1983 Ms 6.8	6.73	
	Balabantaş S	LL+R	260-2	H	59	24	200	234	87	90		25	25		6.90	25;31
	Gaziler S	LL+R	260-3	H		25	202	250	87	90						
Göle F	LL	261	Q		33	186	255	87	90						6.86	25;31
Ağrı EF	NN	262-3	Q		11	0	359	87	90			25	25		6.23	
	NN	262-1	Q		8	304	322	87	90						6.17	
	NN	262-2	Q		9	317	341	87	90						6.23	
Iğdır FZ	RL	263	H		29	295	331	87	90						6.70	8;26;31
Doğubeyazıt F	RL	264	H		20	298	310	87	90					6.62		
Balıgözü FZ	Çandervis S	RL	265-1	H		25	332	355	87	90					6.73	
	Perilidağ S	RL	265-2	H		32	306	339	87	90					6.85	
	Kovancık S	RL	265-3	H	95	10	295	308	87	90		25	25		6.28	8;26;31
	Tirso Gölü S	RL	265-4	H		30	290	333	87	90						
	Yeniçadır S	RL	265-5	H		17	297	314	87	90					6.20	
	Çetenli S	RL	265-6	H		18	284	320	87	90					6.52	
Tendürek EF	NN	266	H		11	325	358	87	90					6.33	8;26;31	
Diyadin EF	NN	267	H		4	315	340	87	90					5.83		
Hamur F	LL	268	H		18	5	11	87	90					6.57		
Tutak F	RL	269	H		57	280	315	87	90					7.13		
Unnamed FZ	RL	270	Q		12	107	123	87	90					6.37		
Unnamed F	RL	271	Q		5	295	295	87	90			25	25		5.94	
Kazbel F	RL	272	H		37	275	303	87	90							6.92
Unnamed F	RL	273	Q		9	264	296	87	90					6.23		
Unnamed F	RL	274	Q		6	341	341	87	90					6.03	25;31	
Akdağ F	RL	275	H		20	273	303	87	90					6.62		
Varto FZ	RL	276	ER		45	97	137	87	90					1966a Ms 6.8	7.01	
Yorgaçayırı-Kaynarca Fz	RL	277-1	Q		16	130	130	87	90			25	20		6.51	
	RL	277-2	H		26	285	330	87	90						1966b	7.00

Table 1 continued

Fault				Length (km)	Trend (RHR)		Dip (Degree)		Slip rate (mm/year)		Depth (km)		Magnitude		References
Segment	Type	ID No	AC		Min	Max	Min	Max	Min	Max	1	2	Obs.	Est. Mw	
Kavakbaşı FZ		RL 277-3	Q	9	283	292	87	90					Ms 6.2	6.23	
	Akdoğan Gölü F	RL 278	H	47	201	296	87	90						7.04	
	Unnamed F	RL 279	H	6	278	279	87	90						6.03	
	Unnamed F	R 280	H	4	244	244	25	30						5.73	
	Bulank F	RL 281	H	11	308	333	87	90						6.33	
	Haçlı Gölü F	R 282	H	20	231	262	87	90						6.62	
	Malazgirt F	LL 283	H	21	182	243	87	90						6.64	
	Unnamed F	RL 284	H	5	219	246	87	90			25	25		5.94	
	Süphan F	LL 285	H	13	207	220	87	90						6.41	
	Bulamaç F	RL 286	H	13	304	336	87	90						6.41	
	Unnamed F	LL 287	Q	15	203	211	85	90						6.48	
	Erciş F	RL 288-1	H	30	139	319	87	90						6.81	
		RL 288-2	H	13	275	299	87	90						6.41	
		RL 288-3	H	11	271	310	87	90			25	25		6.33	8:26
		RL 288-4	H	5	273	298	87	90						5.85	
	Çaldıran F	RL 289	ER	52	269	320	87	90					1976 Ms 7.3	7.08	8:26
	Unnamed F	R 290	Q	4	235	235	40	45						5.83	25:31
	Hasantimur Gölü F	RL 291	H	32	311	330	87	90						6.85	
	Dorutay F	RL 292	H	12	300	314	87	90						6.37	
	Saray FZ	RL 293	H	24	254	313	87	90						6.68	8:26
	Başkale F	LL 294	H	48	215	254	87	90			25	25		7.04	
	Van FZ	R 295	ER	27	246	273	40	50					2011 Mw 7.2	6.76	
	Unnamed F	LL 296	Q	4	244	244	87	90						5.65	
	Unnamed F	LL 297	Q	7	192	194	40	55						6.11	
	Nemrut EF	NN 298	H	9	341	350	87	90						6.23	25:31
	Unnamed F	LL+R 299	Q	12	230	256	87	90						6.90	
	Nazik Gölü F	RL 300	H	22	287	307	87	90						6.64	
	Muş FZ	R 301-1	H	36	264	301	40	50						6.40	
R 301-2		H	82	47	237	319	40	50			25	25		7.04	25:31
Yeniköşk F	R 302	H	13	210	281	40	50			25	25		6.60	8:26	
Unnamed F	RL 303	H	8	309	315	87	90			25	18		6.17	25:31	
Kaleköy S	RL 304-1	H	21	298	315	87	90						6.64		
	RL 304-2	H	88	16	296	300	87	90			25	25		6.70	25:31
	RL 304-3	H	45	272	310	87	90						7.01		
Kuşburnu F	RL 305	H	22	104	144	87	90						6.63		
	RL 306	H	21	115	131	87	90			18	18		6.64		
	NN 307	H	10	113	150	65	70			18	15		6.90	5:25:31	
	RL 308	H	29	275	301	87	90			18	25		6.78		
Southeast-Anatolian Thrust Zone	Çubuklu S	R 309-1	Q	35	1	359	40	65			33	25		6.88	25
		R 309-2-1	H	70	216	349	40	65			33	25		6.80	
		R 309-2-2	H	69	252	325	40	65			29	25		7.24	
	Şirvan S	R 309-3-1	H	18	222	289	40	65			25	25		6.53	25:31
		RL+R 309-3-2	H	42	225	295	85	90						6.98	
		R 309-3-3	H	15	223	291	40	65						6.43	
	Kozluk S	R 309-4-1	H	23	260	312	40	65						6.60	
		R 309-4-2	H	19	263	315	40	65						6.80	
		R 309-4-3	H	25	267	318	40	65						6.71	
	Kulp S	R 309-5-1	H	32	249	324	40	65						6.84	
		R+RL 309-5-2	H	43	248	327	40	65						6.99	
	Lice-Dicle S	R 309-6-1	ER	32	239	300	40	65					1975 Ms 6.6	6.84	5:25:31
R 309-6-2		H	30	223	302	40	65						6.80		
R 309-6-3		H	39	251	306	40	65						7.10		
R 309-6-4		Q	27	257	311	40	65						6.75		
R 309-6-5		Q	25	258	3017	40	65						6.71		

Table 1 continued

Fault		Length		Trend (RHR)		Dip (Degree)		Slip rate (mm/year)		Depth (km)		Magnitude		References	
Segment	Type	ID No	AC	(km)	Min	Max	Min	Max	Min	Max	1	2	Obs.		Est. Mw
	Çüngüş S	R	309-7-1	H	34	233	302	40	65					6.87	
		R	309-7-2	H	58	217	256	40	65					7.15	
	Gerger S	R	309-8-1	H	57	229	290	40	65		18	25		7.14	
		R	309-8-2	H	41	245	283	40	65		18	20		6.97	
	Narince S	R	309-9-1	H	34	236	292	40	65					6.87	
		R	309-9-2	H	20	260	321	40	65					6.59	5;25
		R	309-9-3	H	24	250	264	40	65					6.68	
	Işıklar S	R	309-10	Q	23	262	291	40	65		25	25		7.00	25;31
	Konalga S	R+RL	309-11	Q	31	217	285	40	65					6.83	
	Begendik S	R+RL	309-12	Q	30	216	303	40	65					6.81	
Semdinli Yüksekova FZ	Yüksekova S	RL	310-1	H	45	273	327	85	90			25	25	7.02	25
		RL	310-2	H	43	301	321	85	90					6.99	
	Cizre F	R	311-1	H	52	258	305	40	65		25	25		7.08	25
		R	311-2	H	48	261	305	40	65					7.04	
	Unnamed F	RL	312	Q	11	279	292	85	90					6.33	
	Unnamed F	RL	313	Q	11	290	294	85	90					6.33	
	Unnamed F	RL	314	Q	7	289	289	85	90		25	20		5.98	25;31
	Unnamed F	RL	315	Q	16	287	289	85	90					6.45	
	Unnamed F	RL	316	Q	9	314	317	85	90					6.23	
	Karacadağ EF	NN	317	Q	16	180	180	85	90					6.70	
	Karacadağ F	NN+	318	Q	28	102	148	85	90		18	20		6.48	5;25;31
	Günaşan F	RL	319	Q	15	99	128	85	90					6.41	
Harran FZ	NN	320-1	Q	9	158	182	65	70					6.23		
	NN	320-2	Q	24	178	196	65	70					6.71		
	NN	320-3	Q	12	168	197	65	70					6.37		
Bozava F	RL+R	321	Q	50	289	312	87	90					7.06		
Besni F	LL	322	H	19	54	61	87	90		18	15		6.55	5	
Antakya FZ	LL+N	323	H	43	196	236	70	80		18	20		6.70		
Reyhani F	RL	324	H	20	116	116	85	90		18	15		6.58	9	
Amik Gölü F	NN	325	H	12	278	333	70	80					6.28		
Dead Sea FZ	Narlı S	NN	326-1	H	25	169	215	80	85					6.73	
	Sakçagöz S	NN+	326-2	H	16	205	243	80	85	2	2	18	18	7.30	
	Yesemek S	LL	326-3-1	H	57	178	190	87	90					7.13	
		LL	326-3-2	H	54	180	211	87	90					7.10	9
	Hacıpaşa S	LL	326-4	H	34	178	194	87	90	5	5	18	20	6.88	
	Armanaz S	LL	326-5	H	25	191	191	87	90					6.10	
	Sermada S	LL	326-6	H	35	223	223	87	90					6.90	
	Afrin S	LL	326-7	H	44	190	200	87	90					7.03	
	Tendürek F	NN	327-1	H	8	289	350	85	90		18	25		6.05	8;26
		NN	327	H	6	272	289	85	90					5.89	
Sıcaçermik EF	NN	328	H	5	1	359	85	90		18	15		7.20	29	

RHR right hand rule, F fault, S segment, FZ fault zone, GS graben system, RL right lateral, LL left lateral, NN normal, R reverse, EF; Extensional fissure; H, Holocene; Q, Quaternary; ER, Earthquake rupture, Obs. observed, Est. Mw. estimated magnitude, Depth (1), Seismogenic thickness based on focal depth; Depth (2), Seismogenic thickness based on literature

Numbers reference for slip-rate and depth; **1** Aktar et al. (2000), **2** Aktuğ et al. (2013), **3** Aktuğ et al. (2009), **4** Akyol et al. (2006), **5** Bulut et al. (2012), **6** Çakir et al. (2003), **7** Djamour et al. (2011), **8** Elliott et al. (2013), **9** Ergin et al. (2004), **10** Ergin and Aktar (2009), **11** Ergintav et al. (2014), **12** Flerit et al. (2004), **13** Karabulut et al. (2002), **14** Kaypak and Eyidoğan (2005), **15** McClusky et al. (2000), **16** Meade et al. (2002), **17** Nyst and Thatcher (2004), **18** Özalaybey et al. (2002), **19** Reilinger et al. (2006), **20** Sato et al. (2004), **21** Tan (2012), **22** Tatar et al. (2012), **23** Tezel et al. (2010), **24** Tiryakioğlu et al. (2013), **25** Türkelli et al. (2003), **26** Utukcu (2013), **27** Vernant et al. (2004), **28** Yavasoglu et al. (2011), **29** Yolsal-Çevikbilen et al. (2012), **30** Zhu et al. (2006), **31** Zor et al. (2003)

Based on GPS data (McClusky et al. 2000; Reilinger et al. 2006), slip rate along the fault zone is ~ 10 mm/year. Approximately, 2/3 of the slip is estimated to be along the southern strand with the rest along the northern strand of the EAF (Duman and Emre 2013). Geological slip rate for the fault zone is proposed as 8.3 mm/year (Herece 2008), whereas paleoseismic data on the Pazarcık segment suggests 5.2 ± 0.6 mm/year slip rate (Yönlü 2012). Accordingly, farther west, the slip rate along Karasu through the southern strand is estimated to diminish to 4.0 mm/year (Şaroğlu et al. 1992a, b; Westaway and Arger 1996; Westaway 2003, 2004; Herece 2008) due to slip partitioning between the Amanos segment of the EAF and the northernmost segments of the DSF zone (Duman and Emre 2013).

Exhaustive GPS velocities have been provided for the segments along SMF zone. However, Duman and Emre (2013) proposed a total of ~ 3 mm/year slip rate which is partitioned throughout the fault segments in the zone based on the systematic offsets within the Holocene drainage network.

4.2 Eastern Anatolia

Eastern Anatolia defines the area between the Southeast Anatolia thrust to the south and the Caucasus thrust belt to the north, and to the east of the Karlıova triple junction (Şengör 1980). The region is under a N–S compressional tectonic regime due to ongoing northward motion of the Arabian plate (Şengör 1980; Şengör et al. 1985; Şaroğlu and Güner 1981; Şaroğlu 1985). Recent deformations in Eastern Anatolia are accommodated by strike-slip faults oriented NW–SE and NE–SW, thrust/reverse faults oriented E–W and N–S oriented extension fissures or normal faults. The strike-slip faults display a conjugate pattern in which NW trending faults are right lateral, NE trending faults left lateral (Şengör et al. 1985; Şaroğlu 1985), however, right lateral faulting is dominant. On the other hand, some of these strike-slip faults have formed multi-segmented large fault systems in the region such as the Balıkgözü (265), Erzurum (257) and Şemdinli–Yüksekova (310) fault zones (Fig. 3).

In the conjugate pattern, major left-lateral strike-slip faults mapped in the region are the Çat fault zone (255), Palandöken fault (256), Erzurum fault zone (257), Haçlıgözü fault (282), Malazgirt fault (283), Süphan fault (285), Erciş fault (288) and Başkale fault (294) (Fig. 3).

The mapped right-lateral strike-slip faults in this region exceed the left-lateral faults both in number and length. These are; the Taşlıçay fault zone (247), Tercan fault (249), Kandilli fault (254), Karayazı fault (259), Iğdır fault zone (263), Doğu Bayazıt fault (264), Balıkgözü fault zone (265), Tutak fault (269), Kazbel fault (272), Akdağ fault (275), Varto fault zone (276), Yorgançayırı–Kaynarca fault zone (277), Akdoğan Lake fault (278), Bulanık fault (281), Ercis fault (288), Çaldıran fault (289), Hasan Timur Lake fault (291), Dorutay fault (292), Saray fault zone (293), Kavakbaşı fault (304), Kuşburnu fault (305), Yenisu fault (306), Yayla fault (308) and Şemdinli–Yüksekova fault (310) zone (Fig. 3).

Thrust or reverse faults are typically E–W oriented. These include the Horasan–Şenkaya fault zone (260), Pasinler fault zone (258), Van fault zone (295), Nazik Gölü fault (300), Muş fault zone (301) and Yeniköşk (302) fault (Fig. 3). Intra-mountain basins which are characteristic tectono-geomorphic elements of the Eastern Anatolia tectonic province have developed along the major thrust fault zone such as Muş, Lake Van and Pasinler basins (Şaroğlu and Güner 1981; Şaroğlu 1985).

Ağrı (262), Tendürek (266), Diyadin (267) and Nemrut (298) extension fissures (Fig. 3) parallel to the compression orientation are considered as active structural features causing

Quaternary volcanic activities in the region (Şaroğlu and Yılmaz 1986; Yılmaz et al. 1998). Details of the surface ruptures developed by four large earthquakes within the last century are well-known (Emre et al. 2013 and references therein). These are the 1966 Varto (Ms 6.8), 1976 Çaldıran (Ms 7.3), 1983 Horasan–Narman (Ms 6.8), and 2011 Van (Mw 7.2) earthquakes. Fault related geomorphic features and historical records reveal that the faults in the region have produced large earthquakes resulted in surface ruptures in the past (Ambraseys and Jackson 1998), however, historical surface faulting was only confirmed on the Erzurum fault zone by paleoseismological investigations (Emre et al. 2004).

4.3 South-east Anatolia thrust zone and foreland

During the Middle-Late Miocene (Langian–Serravalian) the Arabian and Eurasian plates collided along the Bitlis–Zagros suture zone (Şengör and Yılmaz 1981). This resulted in the up-lift of suture zone mountains and transformation of shallow marine environments into molasse basins (Yılmaz 1993). The Bitlis suture is a complex continent-ocean and continent–continent collision boundary starting from southeast Turkey and extending to the Zagros Mountains in Iran (Şengör and Yılmaz 1981; Hempton 1985; Yılmaz 1993; Yılmaz et al. 1993; Şengör 1979a, b, Şengör et al. 1985; Yiğitbaş and Yılmaz 1996).

Tectonic features within this E–W trending thrust belt also get younger from north to south, where the youngest faults are situated along the frontal thrust. En-echelon folds parallel to the general orientation of the main thrust zone are observed through the foreland during field studies; we infer that those frontal folds are associated with the blind thrust faults at depth in the foreland.

The thrust belt is characterized by low-angle thrust faults. The length of the thrust belt between Kahramanmaraş and Hakkari within Turkish borders is more than ~600 km. The thrust zone displays south-facing arc geometry parallel to the Bitlis suture zone. The apex of this arc which is an indicator for the northernmost edge of the Arabian plate in the suture zone is located just south of Karlıova triple junction. Thus, it can be speculated that the Karlıova triple junction forming the eastern tip of the Anatolian micro-plate was formed at the apex of the South-east Anatolia Thrust Zone (SEATZ).

The SEATZ is cut by the EAF at its western limit. To the west of Siirt, its youngest faults along the thrust-front structurally separate the allochthonous in the north and the Arabian autochthonous units in the south (Şengör and Yılmaz 1981; Yılmaz 1993). To the east of Siirt the thrust-front trends NW–SE and becomes a wider deformation zone with a right lateral strike-slip component including the Cizre thrust fault and some right lateral strike-slip faults (Fig. 3). Even though the faults along the western half of the thrust-front are constrained to a narrow zone, to the east they are dispersed over a wider zone.

Considering fault geometry and structural gaps, the SEATZ was divided into 12 fault segments (Fig. 3; Table 1). These segments consist of fault clusters reaching up to 25–50 km width with a braided-pattern. The fault clusters to the west of the apex of the thrust zone are characterized by left-stepping geometries, while the clusters to the east are right-stepping (Fig. 3). The only mapped surface rupture within the SEATZ is associated with the 1975 Lice (Ms 6.6) earthquake (Arpat 1977) (Fig. 3).

To the south of the SEAT, in the southeastern Anatolian province, few Quaternary active faults were mapped. In the regional framework, these faults display conjugate pattern. These include the right lateral strike-slip Bozova fault (312), the left lateral Besni fault (322), the Karacadağ extension fissure (318) and normal faults in the Akçakale graben (320) (Fig. 3; Table 1). Although the area is characterized by weak seismicity, there is no clear evidence for Holocene surface rupturing along these structures.

4.4 Central Anatolia

Central Anatolia in this study defines the area between the NAF and EAF zones to the east of the Eskişehir fault and Tuzgözü fault zone (Fig. 1). The area is characterized by NE–SW trending strike-slip fault splays bifurcating from the NAF system in a fish bone pattern (Şengör et al. 1985; Şengör and Barka 1992) (Fig. 3). However, there are a few individual fault segments with NW trend in the western part of this region.

The splay fault system regionally is divided into two groups based on their orientation and sense of lateral motion. Recent tectonic deformations in the region between the Kızılırmak River and the NAF are accommodated by right lateral strike-slip faults extending subparallel to the main strand of the NAF in an ENE–WSW orientation (Şengör et al. 1985, 2005; Şaroğlu et al. 1987; Koçyiğit and Özacar 2003; Emre et al. 2013). These are the Merzifon–Esençay fault (186), Sungurlu fault (188), Turhal fault (190), Almus fault (191), Gökçe fault (192), Kazankaya fault (193), Çekerek fault (194) and Buğdaylı fault (195) (Fig. 3). These faults extend SW into the Anatolian plate for hundreds of kilometers in compliance with the concave geometry of the NAF zone along in its western continuation (Bozkurt and Koçyiğit 1995).

In the area between the Akdağmadeni fault and the EAF, recent crustal deformations are accommodated by left lateral strike-slip faults conjugate to the NAF and sub-parallel to the EAF transform systems, respectively. Western extensions of those faults traverse the Taurus orogenic belt. Of these, the Central Anatolian fault system (Koçyiğit and Beyhan 1998) formed by the Ecemiş (207), Erciyes (204) and Deliler (202) faults is the largest inner tectonic structure of Central Anatolia. The Deliler fault extends to the Munzur Mountain with a plain geometry where it merges with the Ovacık (233) and Malatya (232) faults forming a fault complex in the Kemaliye fault junction (Fig. 3). The Ovacık fault in the east end of this fault complex is bounded by the Munzur Mountain and merges to the NAF east of the Erzincan basin. The Malatya fault in the south connects to the EAF zone at the Nurhak fault complex (Duman and Emre 2013). The Sarız fault (211), which exhibits similar geometry to these faults extends parallel to the EAF system through the NE tip of the central Taurides, and finally terminates within the Tauride mountain belt by (Fig. 3).

Easternmost central Anatolia between the Erzincan and Bingöl basins and the Karlıova triple junction corresponding to eastern tip of Anatolian micro-plate is characterized by intensive large and small strike-slip faults in a conjugate pattern similarly to East Anatolia. Strike-slip faults are right and left lateral parallel to the NAF and EAF systems, respectively. The right lateral strike-slip Nazimiye fault (236) is the largest fault segment in this region.

In addition to the above mentioned faults, several active faults were mapped in northwest Central Anatolia. The Orta fault (162), Çankırı (185) and Karakeçili faults (183) are examples of such features (Fig. 3). Latter two faults are transpressional structures, are dominantly reverse faults forming a link between the Tuzgözü fault and the Merzifon–Esençay fault splay, which bifurcates from the NAF system.

In central Anatolia, two large earthquakes causing surface faulting occurred in the twentieth century. These are the 1938 Kırşehir earthquake (Ms 6.8) originating from the right lateral strike-slip Akpınar fault (Arni, 1940) and very thin surficial fissures associated with the Orta earthquake (Mw 6.0) in 2000 on the left lateral strike-slip Orta fault which extends conjugate to the NAF (Emre et al. 2001; Taymaz et al. 2001).

4.5 Western Anatolia horst-graben systems

Western Anatolia horst-graben system with an annual GPS velocity of 20 mm/year is one of the most rapid extensional tectonic regions in the world (Aktuğ et al. 2009). This region defines the area bounded by the transtensional right lateral strike-slip Simav fault along the north and the transtensional Burdur–Fethiye zone to the east (Figs. 1, 3). In terms of E–W prolongation, the horst-graben systems are located in-between Isparta Angle and the Aegean Sea (Figs. 1, 3). The Gediz, Büyük Menderes, Denizli, Acıgöl, Çivril–Dinar and Burdur grabens are the most prominent geomorphic features of the region (Fig. 3). Of these, the Gediz and Büyük Menderes graben systems which are the two largest morphotectonic elements of the western Anatolia extensional tectonic regime (Şengör 1982; Paton 1992; Yılmaz et al. 2000) are located in the core of the Menderes Metamorphic Complex (Seyitoğlu et al. 1992; Bozkurt 2001). In the plan view these two graben systems exhibit a symmetric pattern (Fig. 3). Both graben systems are characterized by a low angle detachment fault and several synthetic and antithetic faults on the hanging block of the detachment faults (Şengör 1982, 1987; Bozkurt 2001; Gürer et al. 2001, 2016).

The 170 km-long Büyük Menderes Graben System (BMGS) between the Aegean Sea coast and Denizli graben extends in E–W orientation. Its surface trace presents a west-facing “V” geometry (Fig. 3). The low angle detachment fault is formed along the northern boundary of the graben. The low-angle detachment is overlaid by a high-angle synthetic fault zone reflecting late Quaternary–Holocene activity of the low angle detachment at depth. The northernmost fault of the BMGS was divided into 6 segments based on relay ramps and sharp changes or bends in the orientation of the detachment fault (Fig. 3; Table 1). Fault related morphology, historical records and paleoseismological data reveal the late Holocene activity of the fault zone (Ambraseys and Finkel 1987; Altunel 1999; Yönlü et al. 2010; Sümer et al. 2013). On the other hand, along the southern margin of the graben, there is no clear geomorphic evidence for Holocene activity of faults corresponding to simple antithetic faults in the graben system. We infer that the slip rate of these faults is smaller than the sedimentation rate, and therefore, geological and geomorphological evidence for fault activity were buried due to rapid sedimentation along the Büyük Menderes River (Kazancı et al. 2009).

The 150 km-long Gediz Graben System (GGS) with a general NW–SE trend displays more complex tectonic structure than the BMGS. Active faults of the GGS graben consist of a low angle detachment fault forming the southern boundary, a synthetic fault zone accompanying the detachment and an antithetic northern boundary fault zone (Koçyiğit et al. 1999; Emre et al. 2013). Even though the entire graben system is prone to intense seismicity, only the 1969 Alaşehir earthquake (Ms 6.9) was the only event in the twentieth century known to have produced surface faulting within GGS (Arpat and Bingöl 1969). The graben system is divided into eastern and western parts based on overall fault geometry and spatial distribution (Fig. 3). The faults along the eastern part between Sarıgöl and Salihli are characterized by relatively simple graben geometry.

Towards the west, the graben floor gets wider and reaches a maximum width of 70 km between Dağkızılca and Akhisar. To the west, southernmost fault zone of the graben system splits into 3 branches forming the Manisa, Kemalpaşa and Armutlu fault segments (Emre et al. 2005a, b) (Fig. 3; Table 1). The southern detachment fault with south-facing arc geometry extends between Sarıgöl and Dağkızılca. The NW-trending western tip section of the detachment fault (corresponding to segment 44-5 in Fig. 3) turns into an oblique normal fault with a right lateral strike-slip component and then merges to the right

lateral strike-slip Dağkızılca fault. The western tip of the Kemalpaşa fault segment connects to the İzmir fault. To the northwest, between Manisa and Akhisar, the graben floor is characterized by scattered normal faults forming complex sub graben-horsts within the GGS. Finally, to the northwest, the Soma fault zone with a south-facing arc shape connects to the GGS. Faults forming the western tip of the GGS in different orientations are connected to right lateral strike-slip transfer faults between Kuşadası Bay and the Bakırçay graben. The GGS is divided into 17 fault segments excluding the Soma–Kırkağaç fault zone and İzmir fault which are structurally connected to the graben system.

The Eastern tips of the BMGS and GGS are connected to the Denizli Graben which consists of highly segmented normal faults (Koçyiğit 2005). The Acıgöl Graben on the hanging block of the normal dip slip Çivril–Dinar fault system extends as the eastern extension of Denizli graben; and these two present a rift morphology connecting the Büyük Menderes and Çivril graben systems. To the northeast, the southward-concave Çivril Graben (Özalp et al. 2009) is situated with its approximately N–S oriented graben sections connecting to the Acıgöl and Burdur grabens. Farther south, the Gökova fault (62) which bounds the north of the Gulf of Gökova is an important normal fault (Görür et al. 1995; Kurt et al. 1999; Gürer et al. 2013) in southwest Anatolia (Fig. 3).

In this region, right and left lateral strike-slip conjugate faults with NE–SW and NW–SE orientations are found in-between the grabens. The 1969 Alaşehir (Ms 6.9), 1955 Söke (Ms 6.8), 1995 Dinar (Mw 6.4) earthquakes have resulted in surface rupturing in the region (Emre et al. 2013 and references therein). All of these earthquakes were characterized by normal faulting mechanisms (e.g. Eyidoğan and Jackson 1985; McKenzie 1972).

4.6 Northwest Anatolia transition zone

Northwest Anatolia transition zone (NWATZ) describes the area bounded by the plate boundary NAF system to the north and the regional scale large fault bend formed by the Simav, Soma and Zeytinadağ fault zones to the south (Figs. 3, 4). Along the southern boundary, there is a gradual transition from the extensional tectonic regime represented by normal faults to strike-slip faulting. Due to E–W prolongation, the region between the North Aegean Sea and the outer İsparta Angle is characterized by radial extension (Fig. 3). The 205 km-long transtensional right lateral strike-slip Simav fault zone forming the eastern part of the southern boundary extends in a NW–SE orientation and consists of 7 fault segments. Even though small to mid-size recent earthquake with focal mechanisms (Eyidoğan and Jackson 1985; Kartal and Kadıroğlu 2015) showing normal faulting have occurred in the large scale releasing bend (Emre et al. 2012), the geological-geomorphological offsets, GPS and paleoseismological data are evidences for the strike-slip style deformation and recent activity of the entire the Simav fault zone (Konak 1982; Aktuğ et al. 2009; Duman et al. 2013). The Simav fault zone (30) it connects to the Afyon–Akşehir Graben System in the east (Fig. 3).

Recent crustal deformation in the region is controlled by bend kinematics (Emre et al. 2005a, b, c, 2010, 2011a, b). Active faults in the region form large fault bends with E–W orientation and southward concavity (Fig. 4). These orientations are consistent with both the Central Marmara arc of the NAF (Le Pichon et al. 2001) to the north, and the southern boundary fault bend to the south (Fig. 4). From north to south we define three main large fault bends within the transition zone namely the Southern Marmara bend, the Manyas–Bursa double bend and the Balıkesir bend (Fig. 4). Faults trend in NE and NW directions on the western and eastern limbs of the bends, respectively. Within this conjugate pattern the most important deformation feature is the dominant right lateral strike-slip component.

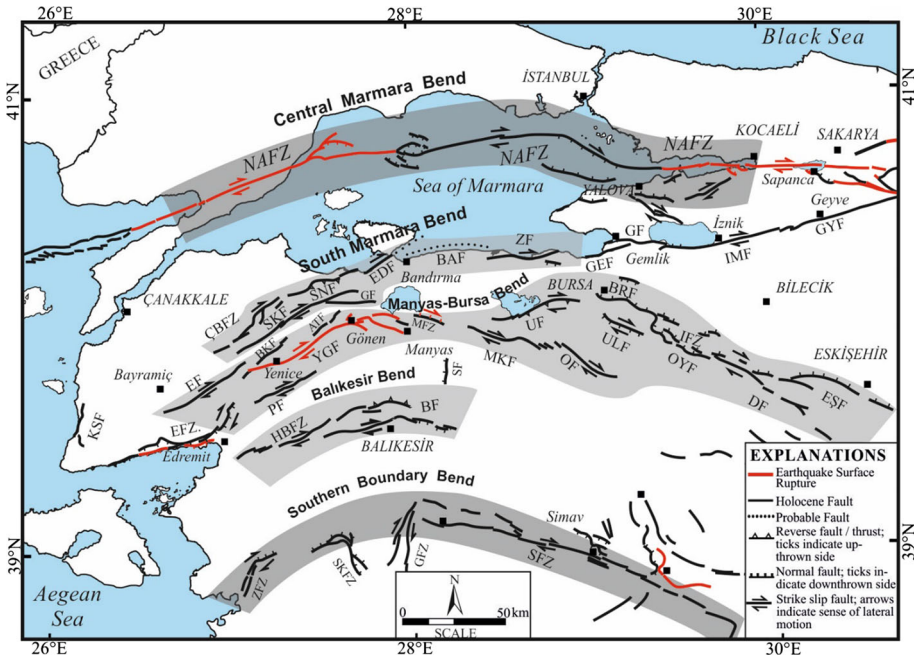


Fig. 4 Fault bend systems in NW Anatolia. Fault bends are parallel to the Central Marmara arc of the North Anatolian fault zone. South Marmara bend corresponds to the western tip of the southern strand of the North Anatolian fault zone. Fault segments of the bends simplified from Emre et al. (2013). *NAFZ* North Anatolian Fault Zone (1), *ZF* Zeytinbağı Fault (11), *BF* Bandırma Fault (10), *EDF* Edincik Fault (9), *SNF* Sinekçi Fault (8), *ÇBF* Çan-Biga Fault Zone (6), *EF* Evciler Fault (4), *YGF* Yenice-Gönen Fault (16), *MFZ* Manyas Fault Zone (17), *MKF* Mustafakemalpaşa Fault (13), *OF* Orhaneli Fault (134), *UF* Uluabat Fault (12), *BRF* Bursa Fault (136), *İFZ* İnegöl Fault Zone (137), *OYF* Oylat Fault (138), *DF* Dodurga Fault (139), *EŞF* Eskişehir fault(140), *HBFZ* Havran-Balya Fault Zone (23), *BAF* Balıkesir Fault (24), *ZFZ* Zeytinadağ Fault Zone, *SKFZ* Soma-Kırkağaç Fault Zone (27), *GFZ* Gelenbe Fault Zone (28), *SFM*, Simav Fault Zone (30), *BKF*, Bekten Fault (19)

However, NE trending faults are transpressional and NW trending faults are transtensional on the western and eastern limbs of the bends, respectively (Fig. 4). Furthermore, it is noted that the normal dip slip component becomes the dominant characteristic of the transtensional faults at the apex of the bends; for example the Manyas and Bursa fault zone along Manyas–Bursa double bend. The Uluabat fault is an example of a transpressional strike-slip fault on the western limb of the bend with a reverse component. On the other hand, towards the southeast, normal dip slip component becomes the dominant characteristic of the faults in the area around Kütahya and Eskişehir (Fig. 4).

The fault bends in the region are multi-segmented fault systems (Figs. 3, 4). The Southern Marmara fault bend consists of the Zeytinbağı (11), Bandırma (10), Edincik (9), Sinekçi (8) and Çan–Biga (6) fault zones. This represents the western continuation of the southern strand of the NAF system (Barka and Kadinsky-Cade 1988) which terminates in the Biga Peninsula (Fig. 4). The Manyas–Bursa double bend is composed of the Evciler (4) Yenice–Gönen fault (16), Manyas fault zone (17), Mustafakemalpaşa fault (13) and Orhaneli (134) faults to the west, and the Uluabat (12), Bursa fault (136) and İnegöl fault zone (137), Oylat fault (138), Dodurga (139) and Eskişehir (140) faults to the east (Fig. 4). To the south, the Balıkesir bend includes the multi-segmented Havran–Balya fault zone

(23) and the Balıkesir fault (24) (Fig. 4). There are also several individual fault segments within the NWATZ. The normal dip slip Edremit fault zone (5) which ruptured in the 1944 earthquake (Ms 6.8) (Ambraseys and Jackson 2000; Emre and Doğan 2010; Sözbilir et al. 2016) and the Kestanbol fault are inconsistent with the bend kinematics in the region. More detailed regional offshore data are needed to understand the normal dip slip kinematic of these faults.

The bend kinematics proposed above are confirmed by slip characteristics of surface ruptures associated with the 1944 Edremit Bay (Ms 6.8), 1953 Yenice–Gönen (Ms 7.2), 1964 Manyas (Ms 7.0) and 1970 Gediz (Ms 7.2) earthquakes in the region (Emre et al. 2013 and references therein).

4.7 Tuzgölü–Konya basin

The Eskişehir and Tuzgölü faults separate the central and western Anatolia tectonic provinces (Barka and Reilinger 1997; Koçyiğit and Özacar 2003) (Figs. 1, 3). Different researchers have proposed various kinematic attributes for the Tuzgölü fault. For instance, Şaroğlu et al. (1987, 1992a, b) suggests a right-lateral fault according to systematic offsets in the late Quaternary lava flows from the Hasandağı volcanic center eruptions, whereas Barka and Reilinger (1997) propose a right-lateral faulting mechanism with a reverse component (Şengör et al. 1985). Recent studies (Emre et al. 2013; Kürçer and Gökten 2014) including detailed mapping and trench surveys clarified that the recent activity is dominated by normal faulting mechanisms.

The 200 km-long Tuzgölü normal fault zone extends in NW–SE orientation and consists of 6 geometric segments. The eastern block displays a distinctive morphology that are consistent with the normal fault mechanism. The Western block as the footwall, hosts the second largest lake of the country, and similar morphologic attributes are observed throughout the Konya basin. The Nasuhpınarı fault, Seyithacı fault, Hotamış fault zone, and Konya fault are Holocene active dip slip normal faults in the Konya basin (Koçyiğit 2005; Emre et al. 2013). Paleoseismological data on the Seyithacı fault reveal that these are low slip-rate normal faults which are capable of producing surface rupturing during the large earthquakes (Özalp et al. 2011).

4.8 Isparta angle

The Isparta Angle (Blumenthal 1963) is an important tectonic structure within the westward escape tectonic regime of the Anatolian plate (McKenzie 1978; Robertson 1998; Koçyiğit and Özacar 2003; Koçyiğit 1983; Şengör et al. 1985; Boray et al. 1985, Taymaz and Price 1992; Barka et al. 1995; Glover and Robertson 1998; Dolmaz 2007; Över et al. 2010; Tiryakioğlu et al. 2013). Its overall geometry is characterized by an upside down “V” shaped, south-facing arc that corresponds to the Sultandağı fault bend (Emre et al. 2002). The 100 km-long Sultandağı fault (Şengör et al. 1985) is the main tectonic element of the Isparta angle. With the exception of Koçyiğit (1983, 1984) and Koçyiğit et al. (2000), most previous works (Şengör et al. 1985; Boray et al. 1985; Barka et al. 1995) including the first edition of the Active Fault Map of Turkey (Şaroğlu et al. 1992a, b) identify the Sultandağı fault as a high angle reverse fault with right lateral strike-slip component. However, surface ruptures associated with the 3rd February 2002 Sultandağı earthquake (Mw 6.5) confirms dip slip normal faulting (Emre et al. 2002) as stated by Koçyiğit (1983). Morphotectonic structures indicating Quaternary–Holocene activity within the Isparta Angle consist of complex horst-grabens. In the regional framework, the

Sultandağı fault (126) is the master fault and drives crustal deformation in the region. The Sultandağı horst bounded by the Sultandağı fault to the north is the most prominent morphotectonic element of the Isparta Angle. It is connected to the Fethiye–Budur zone (Barka et al. 1995) through the Karamuk fault to the west, and the Tuzgözü–Konya basin to the east.

Complex graben systems are the characteristic feature of the Isparta Angle, however, the geometry of the grabens are different along the outer and inner Isparta Angle which are separated from each other by the Sultandağı master fault. Horst and graben structures form a radial pattern on the hanging block of the master fault. The Afyon–Akşehir and Karamuk grabens are parallel to the master fault; whereas numerous NW and/or NE trending cross-grabens and horsts are the perpendicular to the fault bend. The cross-graben and horsts tend to be triangular in map view (Fig. 3). The horst surfaces were tilted far away from their apexes. These regional morphotectonic data indicate crustal stretching in a radial pattern at the apex of Isparta Angle as a result of dome shape uplifting (Emre et al. 2002). Geothermal fields prevailing in the outer Isparta Angle–Afyon–Akşehir graben system—may also be geological evidence for crustal thinning as result of radial stretching in the region. Finally, the counter-clockwise rotation of the Western Anatolia interpreted from GPS vectors (McClusky et al. 2000; Reilinger et al. 1997, 2006; Aktuğ et al. 2009) might have been controlled by radial crustal stretching on the outer Isparta Angle. This would imply regional importance for this tectonic structure in the Eastern Mediterranean.

Except for the Sultandağı master fault, other faults forming the complex Afyon–Akşehir graben system are highly segmented. Faults in this graben system are divided into 14 segments including the master fault (Fig. 3; Table 1). The Sultandağı master fault is divided into six geometric segments (Table 1). Length of the segments varies from 18 to 23 km. The 2002 Sultandağı earthquake (Mw 6.5) occurred at the apex of the Sultandağı fault bend with complex multi-segmented surface rupturing (Emre et al. 2002).

The Plio-Quaternary morphotectonic structures in the inner Isparta Angle are characterized by conjugate grabens (Fig. 3). They are bounded by the dip slip normal faults (numbered from 86 to 95 in Fig. 3) where some of them are reactivated along the paleotectonic thrust faults such as Beyşehir Gölü fault (92) as a result of tectonic inversion.

5 Fault parameters

Several fault parameters are required to characterize linear sources in seismic hazard analysis. Table 1 summarizes fault parameters for the 485 active faults in the Active fault database of Turkey. Faults classified as probable active or lineaments are not included in the table. This table defines following information and parameters; (1) ID numbers, (2) fault/segment name, (3) fault type, (4) activity class, (5) length, (6) trend, (7) attitude, (8) estimated slip rate for the major faults, (9) estimated seismogenic depth and (10) estimated empirical maximum magnitude. The table also includes magnitude of the earthquakes resulting in the surface rupturing since 1900. Fault nomenclature, type and classification were assigned as described in the previous chapters. Each fault segment is defined by an identification (ID) number, with the ID numbers given in Table 1 being consistent with the numbering on Fig. 3. If the fault is a multi-segmented fault system or fault zone the segments are numbered with sub-numbers. For example the Gerede segment of the NAF was defined as ID1-20. In this notation the first number (1) indicate that the fault has multi-segments, a fault system or a zone, the second number indicates the fault segment.

Additionally we defined sub-segments by a third number, however, these sub-segments could not be able to present in given scale of Fig. 3. Thus, we present parameters for 588 fault segments and sub-segments. Segmentation and identification of fault segments are based on the original geometry of the faults on the 1:25,000 scale base maps.

Parameters identified for historical ruptures and Holocene faults such as fault type and segmentation, length, orientation, fault plane dip were verified by field observations. However, it could not have been possible to provide some of the parametric data for Quaternary faults.

Faulting type indicates sense of motion on the fault plane. The faults are defined as; RL, right lateral strike-slip; LL, left lateral strike-slip; NN, normal dip slip; R, reverse or thrust faults. If the fault has oblique slip the first notation indicates the dominant mode of deformation and the second one defines secondary slip. For example the notation RL–NN indicates the fault is a right lateral strike-slip fault with a normal dip slip component.

Fault length defines the total mapped length of the fault or fault segments on the 1:25,000 scale active fault maps. The length of the single fault segments correspond to the map view of the fault. However the total length of the multi-segmented fault may be different depending on the geometry of jog structure. GIS analyses were utilized in order to identify precise lengths of fault segments.

The strike is defined according to the right-hand rule. Based on bend geometry, reverse and normal components were considered on strike-slip faults. Dips of the fault planes were mainly based on field observation and measurements. If available fault plane solutions of earthquakes were also considered. We summarize the other fault parameters defined in the study below.

5.1 Slip rate

Fault slip rate is an important parameter for evaluating the seismic hazard potential of active fault zones. Long-term and short-term slip rate or surface motions are determined by means of geologic, geomorphic and geodetic surveys, respectively. In the study region, geologically determined slip-rates of the major active faults are relatively well known (e.g. Bozkurt 2001 and references therein; Duman and Emre 2013,) but, the data supporting geological slip-rates for the less active faults is sparse. Substantial progress has been made on geodetic surveys of motions within plate interiors (Meade et al. 2002; Flerit et al. 2004; Kadirov et al. 2008; Aktuğ et al. 2009, 2013; Djamour et al. 2011) in addition to those occurring at plate boundaries (e.g. McClusky et al. 2000; Reilinger et al. 2006). Additionally there is reasonable agreement between recent geologic (2–3 Ma) and geodetic plate motion estimates for the last 20 years, (e.g. Bozkurt 2001; Reilinger et al. 2006; Duman and Emre 2013).

The updated active fault geometry presented in this study reveals that the neotectonic provinces of Turkey are divided into blocks bounded by long, multi-segmented fault zones. There is a reasonable agreement between the block boundaries developed from GPS studies and the main fault zones of the Active Fault Map of Turkey, and some block models were suggested for Turkey and its surroundings (McClusky et al. 2000; Nyst and Thatcher 2004; Reilinger et al. 2006; Aktuğ et al. 2009, 2013). In reality the deformation zones along block boundary faults are far more complex than the general understanding provided by GPS studies. Within the Anatolian plate and Eastern Anatolia the block boundaries are represented by wide and complex deformation zones including many fault segments. Consequently; it is not yet possible to assign geodetic slip rates for all the faults

identified. However, we have defined slip rate for major fault systems based on available data (Table 1).

5.2 Seismogenic depth

Even though earthquakes in Turkey are usually characterized by shallow-depth earthquakes in the crust, significant variances are observed in seismogenic depths (Duman et al. 2016). This is related to variations in the lithospheric composition of the crustal structure, existence of suture zones juxtaposing different lithospheric components and variations in the mechanisms of active tectonics around Turkey. In general, seismogenic depth increases from west to east and north to south.

Northern Anatolia, is typically represented by earthquakes generated by the NAF system, from west to east, the seismogenic zone slightly increases from ~ 17 to 20 km deep (Kaypak and Eyidoğan 2005; Özalaybey et al. 2002; Çakir et al. 2003; Karabulut et al. 2002). Western Anatolia is characterised by shallow earthquakes ~ 12 –15 km deep (Tezel et al. 2010; Ergin and Aktar 2009; Tan 2012). Central Anatolia experiences deeper earthquakes reaching a depth of ~ 17 –20 km (Yolsal-Çevikbilen et al. 2012; Bulut et al. 2012). Eastern Anatolia is represented by more complicated structure resulting in difference in the seismogenic thickness ranging from 20 to 25 km (Türkelli et al. 2003; Zor et al. 2003; Elliott et al. 2013; Utkucu 2013). Although the seismicity of the EAF zone, SEAT zone, the Karlıova triple junction area and the area east of this junction have similar hypocentres ($h > 20$ km), the seismicity of the EAF zone is typically less than 20 km (Türkelli et al. 2003). However, the main shock of 1998 Mw 6.2 Ceyhan earthquake with a 32 km depth and aftershocks (Aktar et al. 2000) reveal that seismogenic depth become deeper in the Iskenderun Bay where the northern strand of the EAF merges to Cyprus arc. Recent studies on the 2011 Van earthquake resulting from a reverse mechanism have shown the seismicity to more than 20 km depth (Elliott et al. 2013; Utkucu 2013).

Additionally, latest improved instrumental earthquake catalogue was prepared by Kadirioğlu et al. (2016) for Turkey and the surrounding countries. It covers the region between latitudes 32–45°N and longitudes 23–48°E. The catalogue includes 12,674 events for the period between 1900 and 2012. In the catalogue, there is a considerable amount of events occurred before 1960s, which were not well-resolved by the location algorithms (fixed at 33 km) or without depth information (fixed at 10 km) as flag to show that the depths were no good.

We also evaluated focal depths of all earthquakes included in the new earthquake catalogue (Fig. 5). We examined focal depths by distributions of the earthquakes within an 8-km buffer zone of the 485 fault segments (Fig. 6). Based on both available literature and the improved catalogue, we estimated seismogenic depths ranging from 13 to 33 km for the 485 active fault segments of Turkish territory (Table 1).

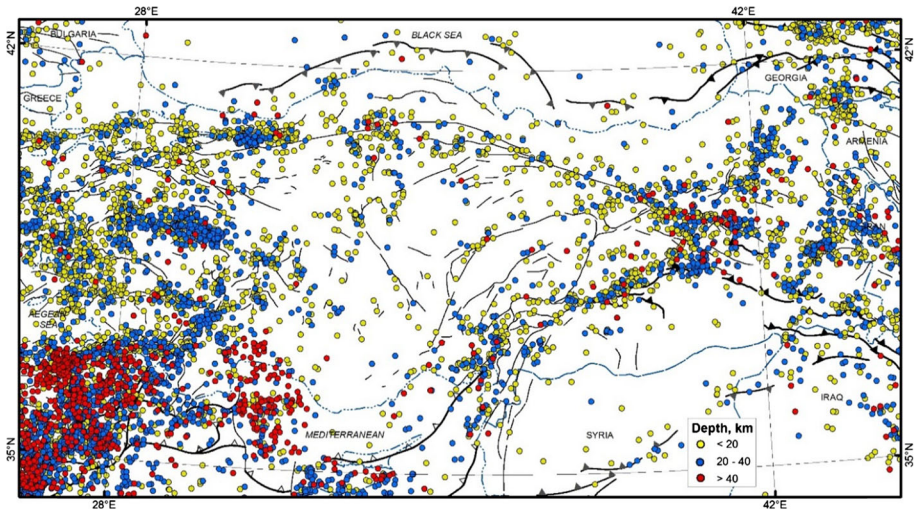


Fig. 5 The distribution of the seismicity according to the focal depth across Turkey and surrounding region, 1900–2012, $M_w \geq 4.0$ (from Duman et al. 2016)

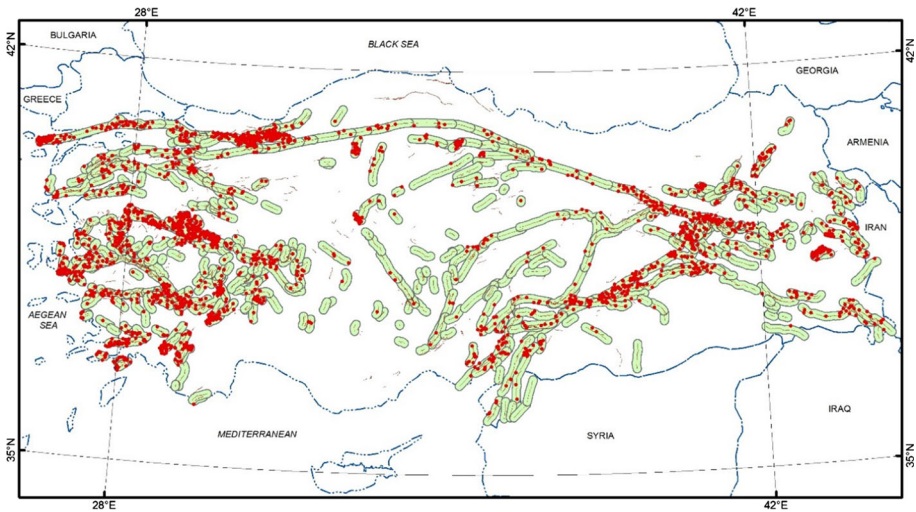


Fig. 6 Spatial distribution of earthquakes from 1900 to 2012 larger than $M_w \geq 4.0$ within the 8-km wide buffer zones of the active faults. Earthquake data was taken from Kadiriöglu et al. (2016)

5.3 Estimated maximum magnitude

During the seismic hazard analysis, it is necessary to estimate maximum earthquake magnitude that might be generated by an individual fault segment. However few large earthquakes are known that occurred during the historical period. Therefore, the expected magnitude scale of a fault segment is commonly evaluated from the fault dimensions, which are associated with earthquake magnitude (Wells and Coppersmith 1994).

Approaches in estimating maximum earthquake magnitudes on individual fault segments typically are based on empirical relationships between magnitude, rupture length, rupture width, rupture area, and surface displacement. These correlations have been investigated by numerous researchers during the last half century (e.g. Bonilla et al. 1984; Darragh and Bolt 1987; Scholz 1982; Slemmons et al. 1989; Stirling et al. 2002; Wells and Coppersmith 1994; Wesnousky 2008). The most common feature that is correlated with magnitude is the surface rupture length as a function of slip type (Wells and Coppersmith 1994). In this study, we calculated maximum magnitudes on fault segments that are individual seismogenic structure from empirical relations between maximum magnitude and surface rupture length inferred by Wells and Coppersmith (1994). The reason for the selection of formulations developed by Wells and Coppersmith (1994) is the inclusion of several surface rupture and earthquake data from Turkey in their database. The estimated maximum moment magnitudes (M_w) of the 554 fault segments range from 5.3 to 8.0 (Table 1). In this table, we have considered only total rupture length associated with the large earthquakes since 1900 such as multi-segmented large earthquakes along the NAF. Proposed estimated magnitudes on the other faults represent individual fault segments. Therefore, we would like to note that logic tree approach is needed for understanding the estimated magnitudes of multi-segmented large fault zones based on the fault geometry and segmentation data including slip rate.

6 Conclusions

In this study, we summarize the development of a new nationwide database of active faults that spans all of Turkey. The database represents our current best understanding of the location, style, and deformation rates of active faults in Turkey. Primary observations from the study are as follows.

- The updated active fault map of Turkey and its database provide the most recent characteristics of seismic sources on a national basis. The map outputs were prepared at three different scales; (1) Base active fault maps of 1:25,000 scale, (2) Active fault map series of Turkey at 1:250,000 scale intending to provide essential fault data for regional earthquake hazard analysis and regional physical planning, and (3) Active fault map of Turkey at 1:1,250,000 scale providing active fault information in order to support hazard mitigation strategies for national policy, strategy, and physical infrastructure planning. All the maps are available on the map portal or web page of the MTA General Directorate.
- Active faults are classified into four distinct types based on geochronological criteria. These are faults with known earthquake surface rupture, Holocene-active faults, Quaternary-active faults and Probable Quaternary-active faults or lineaments.
- The database contains 533 single fault segments ranging between 4 and 330-km, which are substantially potential as earthquake sources.
- The database includes 338 Holocene-active fault segments and 121 Quaternary-active segments. Strike-slip (261; 48.9%) and normal slip (227; 42.5%) faults constitute the majority of fault segments in the database. Fault segments with reverse slip (45; 8.6%) are comparatively few.
- The database includes 28 historical earthquake surface ruptures delineated in detail, which occurred during the last century.

- Fault parameters, which are essential data for seismic hazard analysis, such as class, activity, type, length, trend, and attitude of fault planes were defined for each of the 533 fault segments mapped in Turkey. The parameters have been augmented by estimates of slip-rate, seismogenic depth and expected maximum magnitude based on available data.
- The database provides information in order to support hazard mitigation strategies for national policy, strategy, and physical infrastructure planning and essential fault parameters for regional-scale seismic hazard assessment. Additional evaluations including more detailed consideration of probably Quaternary faults and lineaments will likely be required for site-specific studies of important facilities.

Acknowledgements This work was carried out as the ‘Updating of Active Fault Map of Turkey and its Database’ project supported by the General Directorate of Mineral Research and Exploration (MTA) between 2004 and 2011. We gratefully acknowledge the MTA for the support provided. Also we would like to thank the reviewers for their comments that improved the paper. The active fault base maps are accessible on the Earth Science Map Portal of the MTA (<http://yerbilimleri.mta.gov.tr>).

References

- Aksoy ME, Meghraoui M, Vallee M, Çakır Z (2010) Rupture characteristics of the AD 1912 Murefte (Ganos) earthquake segment of the North Anatolian fault (western Turkey). *Geology* 38:991–994
- Aktar M, Ergin M, Ozalabay S, Tapirdamaz C (2000) A lower-crustal event in the Northeastern Mediterranean: the 1998 Adana Earthquake ($M_w = 6.2$) and its Aftershocks. *Geophys Res Lett* 27(16):2361–2364
- Aktuğ B, Nocquet JM, Cingöz A, Parsons A, Erkan Y, England P, Lenk O, Gürdal MA, Kilicoglu A, Akdeniz H, Tekgül A (2009) Deformation of western Turkey from a combination of permanent and campaign GPS data: limits to block-like behaviour. *J Geophys Res*. doi:10.1029/2008j006000
- Aktuğ B, Parmaksız E, Kurt M, Lenk O, Kılıçoğlu A, Gürdal MA, Özdemir S (2013) Deformation of Central Anatolia: GPS implications. *J Geodyn* 67:78–96. doi:10.1016/j.jog.2012.05.008
- Akyol N, Zhu L, Mitchell BJ, Sözbilir H, Kekovali K (2006) Crustal structure and local seismicity in western Anatolia. *Geophys. J Int* 166:1259–1269
- Altunel E (1999) Geological and geomorphological observations in relation to the 20 September 1899 Menderes earthquake, Western Turkey. *J Geol Soc* 156:241–246
- Ambraseys NN (1970) Some characteristic features of the North Anatolian fault zone. *Tectonophysics* 9:143–165
- Ambraseys NN (1988) Engineering seismology. *J Earthq Eng Str Dyn* 17:1–105
- Ambraseys NN (2002) The seismic activity of the Marmara Sea region over the last 2000 years. *Bull Seismol Soc Am* 92:1–18
- Ambraseys NN, Finkel CF (1987) Seismicity of Turkey and neighbouring regions, 1899–1915. *Ann Geophys* 5B(6):701–726
- Ambraseys NN, Finkel CF (1995) The seismicity of Turkey and adjacent areas: a historical review. Eren Yayıncılık, İstanbul, pp 1500–1800
- Ambraseys NN, Jackson JA (1998) Faulting associated with historical and recent earthquakes in the Eastern Mediterranean region. *Geophys J Int* 133:390–406
- Ambraseys NN, Jackson JA (2000) Seismicity of the Sea of Marmara (Turkey) since 1500. *Geophys J Int* 141:F1–F6
- Angelier J, Lybérís N, Le Pichon X, Barrier E, Huchon P (1982) The tectonic development of the Hellenic arc and the sea of Crete a synthesis. *Tectonophysics* 86:159–196
- Armijo R, Meyer B, Hubert-Ferrari A, Barka A (1999) Westward propagation of the North Anatolian fault into the northern Aegean: timing and kinematics. *Geology* 27:267–270
- Armijo R, Meyer B, Navarro S, King G, Barka A (2002) Asymmetric slip partitioning in the Sea of Marmara pull-apart: a clue to propagation processes of the North Anatolian fault? *Terra Nova* 14(2):80–86
- Armijo R, Pondard N, Meyer B, Uçarkus G, Mercier de Lepinay B, Malavieille J, Dominguez S, Gustcher MA, Schmidt S, Beck C, Çagatay N, Çakır Z, Imren C, Eris K, Natalin B, Özalaybey S, Tolun L, Lefevre I, Seeber N, Gasperini L, Rangin C, Emre O, Sarikavak K (2005) Submarine fault scarps in the

- Sea of Marmara pull-apart (North Anatolian fault): implications for seismic hazard in Istanbul. *Geochem Geophys Geosyst* 6(6):1–29. doi:[10.1029/2004GC000896](https://doi.org/10.1029/2004GC000896)
- Arpat AE (1971) 22 Mayıs, 1971 Bingöl Depremi-Ön Rapor. Institute of Mineral Research and Exploration Report No: 4697
- Arpat E (1977) 1975 Lice depremi. *Yeryuvarı ve İnsan* 2–1:15–27
- Arpat E, Bingöl E (1969) Ege bölgesinin gelişimi üzerine düşünceler. *Min Res Bull* 73:1–9
- Arpat E, Şaroğlu F (1972) Doğu Anadolu Fayı ile ilgili bazı gözlemler ve düşünceler. *MTA Dergisi* 78:33–39
- Arpat E, Şaroğlu F (1975) Türkiye’deki bazı önemli genç tektonik olaylar. *Türkiye Jeoloji Kurumu Bülteni* 18:91–101
- Ayhan ME, Demir C, Kahveci M, Kaplan M (1995) 1990–1993 Yılları GPS ölçümleri ile Gerede-Adapazarı bölgesindeki alanın belirlenmesi. In: *Türk Haritacılığının 100. yılı Bilimsel Kongresi*, pp 55–66, Ankara
- Barka AA (1992) The North Anatolian fault. *Ann Tecton* 6:174–195
- Barka AA (1996) Slip distribution along the North Anatolian fault associated with the large earthquakes of the period 1939 to 1967. *Bull Seismol Soc Am* 86(5):1238–1254
- Barka A (1997) Neotectonics of the Marmara region in active tectonics of northwest Anatolia. In: Schindler C, Pfister M (eds) *The Marmara poly-project*. Hochschulverlag AG and der ETH, Zurich, pp 55–87
- Barka AA, Kadinsky-Cade K (1988) Strike-slip fault geometry in Turkey and its influence on earthquake activity. *Tectonics* 7:663–684
- Barka A, Reilinger R (1997) Active tectonics of the Eastern Mediterranean region: deduced from GPS, neotectonic and seismicity data. *Anali di Geofisica* 40(3):587–610
- Barka A, Reilinger R, Şaroğlu F, Şengör AMC (1995) The Isparta Angle: its importance in the neotectonics of Eastern Mediterranean region. In: *IESCA-1995 Proceedings*, pp 13–18
- Barka AA, Akyüz HS, Cohen HA, Watchorn F (2000) Tectonic evolution of the Niksar and Tasova-Erbaa pullapart basins, North Anatolian Fault Zone: their significance for the motion of the Anatolian block. *Tectonophysics* 322:243–264
- Barka AA, Akyüz S, Altunel E, Sunal G, Çakır Z, Dikbaş A, Yerli B, Armijo R, Meyer B, Chabaliere JB, Rockwell T, Dolan JR, Hartleb R, Dawson T, Christofferson S, Tucker A, Fumal T, Langridge R, Stenner H, Lettis W, Bachhuber J, Page W (2002) The surface rupture and slip distribution of the 17 August 1999 İzmit earthquake (M 7.4), North Anatolian fault. *Bull Seismol Soc Am* 92(1):43–60
- Blumenthal MM (1963) Le système structural du Taurus sud Anatolies. *Bull Soc Geol Fr In: Livre a Memoire de Professor P. Fallot. Mem Soc Geol Fr* 1(2):611–662
- Bonilla MG, Mark RK, Lienkaemper JJ (1984) Statistical relations among earthquake magnitude, surface rupture length, and surface fault displacement. *Bull Seism Soc Am* 74:2379–2411
- Boray A, Şaroğlu A, Emre O (1985) Isparta büyüklüğünün kuzey kesiminde doğu-batı daralma için veriler. *Jeo Müh Dergisi* 23:9–20
- Bozkurt E (2001) Neotectonics of Turkey—a synthesis. *Geodin Acta* 14:3–30. doi:[10.1016/S0985-3111\(01\)01066-X](https://doi.org/10.1016/S0985-3111(01)01066-X)
- Bozkurt E, Koçyiğit A (1995) The Kazova basin: an active negative flower structure on the Almus Fault Zone, a splay fault system of the North Anatolian fault zone, Turkey. *Tectonophysics* 265:239–254
- Bozkurt E, Mittweide SK (2001) Introduction to the geology of Turkey—a synthesis. *Int Geol Rev* 43(7):578–594
- Bulut F, Bohnhoff M, Eken T, Janssen C, Kilic T, Dresen G (2012) The East Anatolian Fault Zone: seismotectonic setting and spatiotemporal characteristics of seismicity based on precise earthquake locations. *J Geophys Res Solid Earth*. doi:[10.1029/2011jb008966](https://doi.org/10.1029/2011jb008966)
- Burchfiel BC, King RW, Todosov A, Kotzev V, Durmurdzanov N, Serafimovski T, Nurce B (2006) GPS results for Macedonia and its importance for the tectonics of the Southern Balkan extensional regime. *Tectonophysics* 413:239–248
- Burke K, Şengör AMC (1986) Tectonic escape in the evolution of the continental crust. In: Barazangi M (ed) *Reflection seismology, continental crust, geodynamic series*. American Geophysical Union Special Publication 14:41–53. doi:[10.1029/GD014p0041](https://doi.org/10.1029/GD014p0041)
- Çakır Z, de Chabaliere JB, Armijo R, Meyer B, Barka AA, Peltzer G (2003) Coseismic and early post-seismic slip associated with the 1999 İzmit earthquake (Turkey), from SAR interferometry and tectonic field observations. *Geophys J Int* 155:93–110
- Caputo R, Chatzipetros A, Pavlides S, Sboras S (2012) The Greek database of seismogenic sources (GReDaSS): state-of-the-art for northern Greece. *Ann Geophys* 55(5):859–894. doi:[10.4401/ag-5168](https://doi.org/10.4401/ag-5168)
- Caputo R, Sboras S, Pavlides S, Chatzipetros A (2015) Comparison between single-event effects and cumulative effects for the purpose of seismic hazard assessment. A review from Greece. *Earth Sci Rev* 148:94–120

- Çetin H, Güneşli H, Mayer L (2003) Paleoseismology of the Palu-Lake Hazar segment of the East Anatolian fault Zone, Turkey. *Tectonophysics* 374:163–197
- Cormier MH, Seeber L, McHugh CMG, Polonia A, Çağatay N, Emre Ö, Gasperini L, Görür N, Bortoluzzi G, Bonatti E, Ryan WBF, Newman KR (2006) North Anatolian fault in the Gulf of İzmit (Turkey): Rapid vertical motion in response to minor bends of a nonvertical continental transform. *J Geophys Res* 111:B04102. doi:10.1029/2005JB003633
- Darragh RB, Bolt BA (1987) A comment on the statistical regression relation between earthquake magnitude and fault rupture length. *Bull Seism Soc Am* 77:1479–1484
- de Polo CM, Clark DG, Slemmons DB, Ayman WH (1989) Historical Basin and Range Province surface faulting and fault segmentation. In: Schwartz DP, Sibson RH (eds) *Fault segmentation and controls of rupture initiation and termination*. US Geol Surv Open File Rep No: 89-315, pp 131–162
- de Polo CM, Clark DG, Slemmons DB, Ramelli AR (1991) Historical surface faulting in the Basin and Range Province, western North America—implications for fault segmentation. *J Struct Geol* 13:123–136
- Dewey JW (1976) Seismicity of Northern Anatolia. *Bull Seismol Soc Am* 66(3):843–868
- Dewey JF, Hempton MR, Kidd WSF, Şaroğlu F, Şengör AMC (1986) Shortening of continental lithosphere: the neotectonics of Eastern Anatolia—a young collision zone. *Geol Soci* 19:1–36. doi:10.1144/gsl.sp.1986.019.01.01
- Djamour Y, Vernant P, Nankali HR, Tavakoli F (2011) NW Iran-Eastern Turkey present-day kinematics: results from the Iranian permanent Gps network. *Earth Planet Sci Lett* 307:27–34
- Dolmaz MN (2007) An aspect of the subsurface structure of the Burdur-Isparta area, SW Anatolia, based on gravity and aeromagnetic data, and some tectonic implications. *Earth Planets Space* 59:5–12
- Duman TY, Emre O (2013) The East Anatolian fault: geometry, segmentation and jog characteristics. *Geol Soc* 372:495–529. doi:10.1144/sp372.14
- Duman TY, Emre Ö, Doğan A, Özalp S (2005) Step-over and bend structures along the 1999 Düzce earthquake surface rupture, North Anatolian fault, Turkey. *Bull Seismol Soc Am* 95:1250–1262
- Duman TY, Elmacı H, Özalp S, Olgun Ş, Emre Ö (2013) Simav Fay Zonunda ilk paleosismolojik bulgular. 66. Türkiye Jeoloji Kurultayı, 1–5 Nisan 2013, ODTÜ Kültür ve Kongre Merkezi, Bildiri Özleri Kitabı, pp 28–29, Ankara
- Duman TY, Çan T, Emre Ö, Kadıroğlu FT, Başarır Baştürk N, Kılıç T, Arslan S, Özalp S, Kartal RF, Kalafat D, Karakaya F, Eroğlu Azak T, Özel NM, Ergintav S, Akkar S, Altınok Y, Tekin S, Cingöz and Kurt Aİ (2016) Seismotectonics database of Turkey. *Bull Earthq Eng*. doi:10.1007/s10518-016-9965-9
- Elliott J, Copley A, Holley R, Schärer K, Parsons B (2013) The 2011 Mw 7.1 Van (Eastern Turkey) earthquake. *J Geophys Res Solid Earth* 118:1619–1637. doi:10.1002/jgrb.50117
- Emre Ö (2010) Türkiye Diri Fay Haritası 1:250.000 Ölçekli Çanakkale (NK 35-10b) Paftası. MTA 1:250.000 Ölçekli Diri Fay Haritaları Serisi, No: 1, 40 s., Ankara, Türkiye
- Emre Ö, Doğan A (2010) Türkiye Diri Fay Haritası 1:250.000 Ölçekli Ayrıvalık (NJ 35-2) Paftası. MTA 1:250.000 Ölçekli Diri Fay Haritaları Serisi, No: 2, 32 s., Ankara, Türkiye
- Emre Ö, Duman TY, Doğan A, Özalp S (2002) 06 Haziran 2000 Orta (Çankırı) Depremi: kaynak fay ve hasar dağılımına etki eden jeolojik faktörler. 54. Türkiye Jeoloji Kurultayı, Bildiriler CD'si, Bildiri No: 54–57, Ankara, 7–10 Mayıs 2001
- Emre Ö, Duman TY, Özalp S, Doğan A, Tokay F, Kuşçu İ (2002) Surface faulting associated with the Sultandağı earthquake (Mw 6.5) of 3 February 2002, Southwestern Turkey. *Seismol Res Lett* 74(4):382–391
- Emre Ö, Awata Y, Duman TY (eds) (2003) *Surface Ruptures Associated with the August 17, 1999 İzmit Earthquake*. General Directorate of Mineral Research and Exploration, Special Publications-1, 51-280, Ankara
- Emre Ö, Koehler RD, Hengesh J, Duman TY, Akyüz S, Altunel E, Barka A (2004) Late holocene activity of Erzurum fault zone in Eastern Anatolia, Turkey, GSA 2004, November 7–10 Denver, Abstract No: 59-2
- Emre Ö, Doğan A, Yıldırım C, Şaroğlu F (2005a) Active fault pattern and bend kinematics in NW Anatolia. In: *International Symposium on the Geodynamics of Eastern Mediterranean: active tectonics of the Aegean Region, 15–18 June 2005*, Kadir Has University, Abstracts, p 98, İstanbul, Turkey
- Emre Ö, Doğan A, Özalp S, Yıldırım C (2005b) İzmir yakın çevresinin diri fayları ve 17 Ekim 2005 Sığacık depremleri. *Cumhuriyet Bilim-Teknik*, 29 Ekim 2005, 971, 8–9, İstanbul
- Emre Ö, Doğan A, Özalp S (2005c) İzmir depremlerinin kaynak fay özellikleri. *Cumhuriyet Bilim-Teknik*, 12 Kasım 2005, 973, 18–19, İstanbul
- Emre Ö, Duman TY, Özalp S, Elmacı H (2010) On the source fault of the 8 March 2010 Başyurt–Karakoçan (Elazığ) Earthquake (Mw:6.1). In: *63rd geological congress of Turkey, April 5–9, 2010, Proceedings Book*, pp 36–37, Ankara

- Emre Ö, Doğan A, Özalp S, Yıldırım C (2011a) 1:250.000 Ölçekli Türkiye Diri Fay Haritası Bandırma (NK 35-11b) Paftası. MTA 1:250.000 Ölçekli Diri Fay Haritaları Serisi, Seri No: 3, 55 s., Ankara
- Emre Ö, Doğan A, Özalp S (2011b) 1:250.000 Ölçekli Türkiye Diri Fay Haritası Balıkesir (NJ 35-3) Paftası. MTA 1:250.000 Ölçekli Diri Fay Haritaları Serisi, Seri No: 4, 35 s., Ankara
- Emre Ö, Duman TY, Özalp S, Doğan A (2012) Simav Fayı ve 19 Mayıs 2011 Simav Depremi (Mw: 5.8). 65. Türkiye Jeoloji Kurultayı, 2-6 Nisan 2012, MTA Genel Müdürlüğü Kültür Sitesi, Bildiri Özleri Kitabı, pp 10–11, Ankara
- Emre Ö, Duman TY, Özalp S, Elmacı H, Olgun Ş, Şaroğlu F (2013) Active fault map of Turkey with an explanatory text 1:1,250,000 scale. General Directorate of Mineral Research and Exploration, Special Publication Series 30
- Ergin M, Aktar M (2009) A high-resolution aftershock seismicity image of the 2002 Sultandağı-Çay Earthquake (Mw = 62), Turkey. *J Seismol* 13:633–646. doi:[10.1007/s10950-009-9155-1](https://doi.org/10.1007/s10950-009-9155-1)
- Ergin M, Aktar M, Eyidoğan H (2004) Present-day seismicity and seismotectonics of the Cilician Basin: Eastern Mediterranean Region of Turkey. *Bull Seismol Soc Am* 94:930–939
- Ergintav S, Reilinger RE, Çakmak R, Floyd M, Çakır Z, Doğan U, King RW, McClusky S, Özener H (2014) Istanbul's earthquake hot spots: geodetic constraints on strain accumulation along faults in the Marmara seismic gap. *Geophys Res Lett* 41:5783–5788. doi:[10.1002/2014GL060985](https://doi.org/10.1002/2014GL060985)
- Eriñç S (1953) Doğu Anadolu'nun coğrafyası, İstanbul Univ. Publ. No572, p 124
- Erol O (1983) Türkiye'nin genç tektonik ve jeomorfolojik gelişimi. *Jeomorfoloji Derg* 11:1–22
- Eyidoğan H, Jackson J (1985) A seismological study of normal faulting in the Demirci, Alaşehir and Gediz earthquakes of 1969–70 in western Turkey: implications for the nature and geometry of deformation in the continental crust. *Geophys J R Astr Soc* 81:569–607
- Flerit F, Armijo R, King G, Meyer B (2004) The mechanical interaction between the propagating North Anatolian fault and the back-arc extension in the Aegean. *Earth Planet Sci Lett* 224:347–362. doi:[10.1016/j.epsl.2004.05.028](https://doi.org/10.1016/j.epsl.2004.05.028)
- Garfunkel Z (2014) Lateral motion and deformation along the dead sea transform. In: Garfunkel Z, Ben-Avraham Z, Kağan E (eds) Dead sea transform fault system—reviews. Springer, Berlin, pp 109–150
- Glover C, Robertson AHF (1998) Neotectonic intersection of the Aegean and Cyprus tectonic arcs: extensional and strike-slip faulting in the Isparta Angle, SW Turkey. *Tectonophysics* 298:103–132
- Görür N, Şengör AMC, Sakıncı M, Tüysüz O, Akkök R, Yiğitbaş E, Oktay FY, Barka A, Sarıca N, Ecevitöğlü B, Demirbağ E, Ersoy S, Algan O, Güneysu C, Aykol A (1995) Rift formation in the Gökova region, southwest Anatolia: implications for the opening of the Aegean Sea. *Geol Mag* 132:637–650
- Gudjabadze GE (2003) Geological Map of Georgia 1:500 000. In: Gamkrelidze IP (ed) Georgian State Department of Geology and National Oil Company 'Saknatobi' Tbilisi
- Gürbüz C, Aktar M, Eyidoğan H, Cisternas A, Haessler H, Barka A, Ergin M, Türkelli N, Polat O, Üçer SB, Kuleli S, Baris S, Kaypak B, Bekler T, Zor E, Biçmen F, Yörük A (2000) The seismotectonics of the Marmara region. *Tectonophysics* 316:1–17
- Gürer ÖF, Bozcu M, Yılmaz K, Yılmaz Y (2001) Neogene basin development around Söke-Kuşadası (Western Anatolia) and its bearing on tectonic development of the Aegean region. *Geodin Acta* 14:57–69
- Gürer ÖF, Sanğu E, Özburan M, Gürbüz A, Sarıca-Filoreau N (2013) Complex basin evolution in the Gökova Gulf region: implications on the Late Cenozoic tectonics of Southwest Turkey. *Int J Earth Sci (Geol Rundsch)* 102:2199–2221. doi:[10.1007/s00531-013-0909-1](https://doi.org/10.1007/s00531-013-0909-1)
- Gürer ÖF, Sanğu E, Özburan M, Gürbüz A, Gürer A, Sinir H (2016) Plio-Quaternary kinematic development and paleostress pattern of the Edremit basin, Western Turkey. *Tectonophysics* 679:199–210
- Hempton MR (1985) Structure and deformation history of Bitlis suture near Lake Hazar, southeastern Turkey. *Bull Geol Soc Am* 96:233–243
- Herece E (2008) Doğu Anadolu Fayı (DAF) Atlası. MTA Özel Yayın Serisi, No: 13, 359 s., Ankara
- Hessami K, Jamali F, Tabassi H (2003) Major active faults of Iran. Ministry of Science, Research and technology, International Institute of Earthquake Engineering and Seismology
- Hubert A, Armijo R, King G, Gasse F, Barka AA (1997) Slip rate of the North Anatolian fault, Turkey: Eos (Transactions, American Geophysical Union), v. 78
- Hubert-Ferrari A, Armijo R, King G, Meyer B, Barka A (2002) Morphology, displacement, and slip rates along the North Anatolian fault, Turkey. *J Geophys Res.* doi:[10.1029/2001JB000393](https://doi.org/10.1029/2001JB000393)
- İmren C (2007) Marmara Denizi aktif tektonizmasının sismik yansıma ve derinlik verilerinin incelenmesi. Maden Tetkik ve Arama Genel Müdürlüğü, Monografi Serisi No: 3, 202 s., Ankara
- İmren C, Le Pichon X, Rangin C, Demirbağ E, Ecevitöğlü B, Görür N (2001) The North Anatolian Fault within the Sea of Marmara: a new interpretation based on multi-channel seismic and multi-beam bathymetry data. *Earth Planet Sci Lett* 186:143–158

- Jackson J, McKenzie D (1984) Active tectonics of the Alpine–Himalayan Belt between western Turkey and Pakistan. *Geophys J R Astr Soc* 77:185–264
- Jennings CW (1994) An explanatory text to accompany the fault activity map of California and adjacent areas with locations and ages of recent volcanic eruptions 1:750000 scale. California Department of Conservation Division of Mines and Geology Publications and Information, Geological Data Map No: 6, 92 p., Sacramento, California
- Kadirioğlu FT, Kartal RF, Kılıç, T, Kalafat D, Duman TY, Eroğlu Azak T, Özalp S, Emre Ö (2016) An improved earthquake catalogue ($M > 4.0$) for Turkey and its near vicinity. *Bull Earthq Eng* (accepted)
- Kadirov F, Mammadov S, Reilinger R, McClusky S (2008) Some new data on modern tectonic deformation and active faulting in Azerbaijan (according to Global Positioning System measurements). *Proc Azerbaijan Natl Acad Sci Earth* 1:82–88
- Karabulut H, Bouin M, Bouchon M, Dietrich M, Cournou C, Aktar M (2002) The seismicity in the eastern Marmara sea after the August 17, 1999 Izmit earthquake. *Bull Seism Soc Am* 92:387–393
- Kartal FR, Kadirioğlu FT (2015) 2011–2012 Simav Earthquakes ($M_I = 5.7$, $M_I = 5.0$, $M_I = 5.4$) and relationship with the tectonic structure of the region. *Yerbilimleri* 35(3):185–198
- Kaypak B, Eyidoğan H (2005) One-dimensional crustal structure of the Erzincan basin, Eastern Turkey and relocations of the 1992 Erzincan earthquake ($M_s = 6.8$) aftershock sequence. *Phys Earth Planet Int* 151:1–20. doi:[10.1016/j.pepi.2004.11.009](https://doi.org/10.1016/j.pepi.2004.11.009)
- Kazancı N, Dündar S, Alçicek MC, Gürbüz A (2009) Quaternary deposits of the Büyük Menderes graben in western Anatolia, Turkey: implication for river capture and longest Holocene estuary in Aegean Sea. *Mar Geol* 264(2–3):165–176
- Ketin İ (1948) Über die tektonisch-mechanischen Folgerungen aus den grossen anatolischen Erdbeben des letzten Dezenniums. *Geol Rundsch* 36:77–83
- Ketin İ (1966) Tectonic units of Anatolia (Asia Minor). *Miner Resour Explor Inst Bull* 66:23–34
- Ketin İ (1968) Relations between general tectonic features and the main earthquake regions of Turkey: mineral research and exploration institute of Turkey. *Bulletin* 71:63–67
- Ketin İ (1969) On the North Anatolian fault. *Bull Min Res Explor Inst* 72:1–28
- Knuepfer PLK (1989) Implications of the characteristics of end-points of historical surface fault ruptures for the nature of fault segmentation. In: Schwartz DP, Sibson RH (eds) *Fault segmentation and controls of rupture initiation and termination*. US Geol Surv Open File Rep No: 89-315, pp 193–228
- Koçyiğit A (1983) Hoyran Gölü (Isparta Büklümü) Dolayının neotektoniği. *TJK Bülent* 26:1–10
- Koçyiğit A (1984) Güneybatı Türkiye ve civarının neotektoniği. *Türkiye Joloji Kurumu Bülten* 27:1–16
- Koçyiğit, A (1988a) Tectonic setting of the Geyve basin: age and total displacement of the Geyve fault zone. In: 1987 Melih Tokay Symposium. *METU J Pure Appl Sci* 21:81–104
- Koçyiğit A (1988b) Basic geologic characteristics and total offset of the North Anatolian Fault Zone in Suşehri area, NE Turkey. *METU J Pure Appl Sci* 22:43–68
- Koçyiğit A (1989) Suşehri basin: an active fault wedge basin on the North Anatolian fault zone. *Tectonophysics* 167:13–29
- Koçyiğit A (1990) Tectonic setting of the Gölova basin: total offset of the North Anatolian Fault Zone, E. Pontide, Turkey. *Ann Tecton* 4:155–170
- Koçyiğit A (2005) The Denizli graben-horst system and the eastern limit of western Anatolian continental extension: basin fill, structure, deformational mode, throw amount and episodic evolutionary history, SW Turkey. *Geodin Acta* 18(3):167–208
- Koçyiğit A, Beyhan A (1998) A new intracontinental transcurrent structure: the Central Anatolian Fault Zone, Turkey. *Tectonophysics* 284:317–336
- Koçyiğit A, Özacar A (2003) Extensional neotectonic regime through the NE edge of outer Isparta Angle, SW Turkey: new field and seismic data. *Turkish J Earth Sci* 12:67–90
- Koçyiğit A, Yusufoglu H, Bozkurt E (1999) Evidence from the Gediz Graben for episodic two-stage extension in western Turkey. *J Geol Soc Lond* 156:605–616
- Koçyiğit A, Ünay E, Saraç G (2000) Epipodic graben formation and extensional neotectonic regime in west Central Anatolia and Isparta Angle: a case study in the Akşehir-Afyon graben, Turkey. In: Bozkurt E, Winchester JA, Piper DA (eds) *Tectonics and magmatism in Turkey and the surrounding Area*. J Geol Soc London, Special Publication 173:405–421
- Konak N (1982) Simav dolayının jeolojisi ve metamorfik kayaların evrimi. *İstanbul Yerbilimleri* 3:313–337
- Kondo H, Özaksoy V, Yildirim C, Awata Y, Emre Ö, Okumura K (2004) 3D trenching survey at Demir Tepe site on the 1944 Bolu-Gerede earthquake ruptures, North Anatolian fault system, Turkey. *Seismol Res Lett* 75(2):292
- Koukouvelas IK, Aydın A (2002) Fault structure and related basins of the North Aegean Sea and its surroundings. *Tectonics* 21(5):1046. doi:[10.1029/2001TC901037](https://doi.org/10.1029/2001TC901037)

- Kozacı Ö, Dolan J, Finkel R, Hartleb RD (2007) Late Holocene slip rate for the North Anatolian fault, Turkey, from cosmogenic ^{36}Cl geochronology: implications for the constancy of fault loading and strain release rates. *Geology* 35(10):867–870
- Kozacı Ö, Dolan JF, Finkel RC (2009) A late Holocene slip rate for the central North Anatolian fault, at Tahtaköprü, Turkey, from cosmogenic ^{10}Be geochronology: implications for fault loading and strain release rates. *J Geophys Res* v:114
- Kozacı Ö, Dolan JF, Yönlü Ö, Hartleb RD (2011) Paleoseismologic evidence for the relatively regular recurrence of infrequent, large-magnitude earthquakes on the eastern North Anatolian fault at Yay-labeli, Turkey. *Lithosphere* 3(1):37–54. doi:10.1130/L118.1
- Kürçer A, Gökten YE (2014) Neotectonic-period characteristics, seismicity, geometry and segmentation of the Tuz Gölü fault zone. *Bull Min Res Exp* 149:19–68
- Kurt H, Demirbağ E, Kuşçu İ (1999) Investigation of the submarine active tectonism in the Gulf of Gökova, southwest Anatolia–southeast Aegean Sea, by multi-channel seismic reflection data. *Tectonophysics* 305:477–496
- Kuşçu İ, Okamura M, Matsuoka H, Awata Y (2002) Active faults in the Gulf of İzmit on the North Anatolian Fault, NW Turkey: a high-resolution shallow seismic study. *Mar Geol* 190(1–2):421–443
- Le Pichon X, Chamot-Rooke C, Lallemand S, Noomen R, Veis G (1995) Geodetic determination of the kinematics of Central Greece with respect to Europe: implications for Eastern Mediterranean tectonics. *J Geophys Res* 100:12675–12690
- Le Pichon X, Şengör AMC, Demirbağ E, Rangin C, İmren C, Armijo R, Görür N, Çağatay N, Mercier de Lepinay B, Meyer B, Saatçılar R, Tok B (2001) The active main Marmara fault. *Earth Planet Sci Lett* 192:595–616
- Le Pichon X, Chamot-Rooke N, Rangin C, Şengör AMC (2003) The North Anatolian Fault in the Sea of Marmara. *J Geophys Res* 108(B4):2179. doi:10.1029/2002JB001862
- Litchfield NJ, Van Dissen R, Sutherland R, Barnes PM, Cox SC, Norris R, Beavan RJ, Langridge R, Villamor P, Berryman K, Stirling M, Nicol A, Nodder S, Lamarche G, Barrell DJA, Pettinga JR, Little T, Pondard N, Mountjoy JJ, Clark K (2014) A model of active faulting in New Zealand. *NZ J Geol Geophys* 57(1):32–56. doi:10.1080/00288306.2013.854256
- McCalpin JP (1996) *Paleoseismology*. Academic Press, New York
- McClusky S et al (2000) Global positioning system constraints on plate kinematics and dynamics in the eastern mediterranean and caucasus. *J Geophys Res* 105:5695–5719
- McClusky S, Reilinger R, Mahmoud S, Ben Sari D, Tealeb A (2003) GPS constraints on Africa (Nubia) and Arabia plate motions. *Geophys J Int* 155:126–138. doi:10.1046/j.1365-246X.2003.02023.x
- McKenzie DP (1970) Plate Tectonics of the Mediterranean Region. *Nature* 226:239–243
- McKenzie D (1972) Active tectonics of the mediterranean region. *Geophys J R Astr Soc* 30:109–186
- McKenzie D (1978) Active tectonics of the Alpine–Himalayan belt—the Aegean Sea and surrounding region. *Geophys J R Astr Soc* 55:217–254
- Meade BJ, Hager BH, McClusky SC, Reilinger RE, Ergintav S, Lenk O, Barka A, Özener H (2002) Estimates of seismic potential in the Marmara region from block models of secular deformation constrained by GPS measurements. *Bull Seismol Soc Am* 92(1):208–215
- Nyst M, Thatcher W (2004) New constraints on the active tectonic deformation of the Aegean. *J Geophys Res* 109:B11406. doi:10.1029/2003JB002830
- Okay Aİ, Tüysüz O (1999) Tethyan sutures of northern Turkey. *Geol Soc Lond Spec Publ* 156:475–515. doi:10.1144/gsl.sp.1999.156.01.22
- Okay Aİ, Tüysüz O, Kaya Ş (2004) From transpression to transtension: changes in morphology and structure around a bend on the North Anatolian Fault in the Marmara region. *Tectonophysics* 391:259–282
- Okumura K, Rockwell TK, Duman T, Tokay F, Kondo H, Yildirim C, Ozaksoy V (2003) Refined slip history of the North Anatolian fault at Gerede on the 1944 rupture: Eos (Transactions, American Geophysical Union), v. 84, no. 46, F715
- Oral MB, Reilinger RE, Toksöz MN, Kong RW, Barka AA, Kınık İ, Lenk O (1995) Global positioning system offers evidence of plate motions in eastern Mediterranean. *EOS Transac.* 76(9)
- Över S, Pinar A, Özden S, Yılmaz H, Can U, Kamacı Z (2010) Late Cenozoic stress field in the Cameli Basin, SW Turkey. *Tectonophysics* 492(1–4):60–72
- Özalaybey S, Ergin M, Aktar M, Tapırdamaz C, Biçmen F, Yörük A (2002) The 1999 İzmit Earthquake sequence in Turkey: seismological and tectonic aspects. *Bull Seismol Soc Am* 92:376–386
- Özalp S, Emre Ö, Duman TY, Şaroğlu F, Özaksoy V, Elmacı H, Koç G (2009) Çivril Graben system: morphotectonic structure and active fault characteristics, SW Turkey. 62nd Geological Congress of Turkey, 13–17 April 2009, Abstracts Book-II, pp 794–795, Ankara, Turkey
- Özalp S, Emre Ö, Duman TY, Törk K (2011) Karapınar (Konya) yöresindeki çizgisel uzanımlı yer çatlaklarının kökeni üzerine paleoseismolojik bulgular. *Aktif Tektonik Araştırma Grubu Onbeşinci*

- Çalıştayı (ATAG-15), 19–22 Ekim 2011, Çukurova Üniversitesi, Bildiri Özleri Kitabı, 20–21, Karataş-Adana
- Özalp S, Emre Ö, Doğan A (2013) The segment structure of southern branch of the North Anatolian Fault and paleoseismological behaviour of the Gemlik fault. *NW Anatolia Bull MTA* 147:1–17
- Pamir HN, Ketin İ (1941) Das Anatolische Erdbeben Ende 1939. *Geol Rundsch* 32:278–287
- Papazachos BC, Papaioannou CA (1999) Lithospheric boundaries and plate motions in the Cyprus area. *Tectonophysics* 308:193–204
- Parsons T, Toda S, Stein R, Barka AA, Dieterich J (2000) Heightened odds of large earthquakes near Istanbul: an interaction-based probability calculation. *Science* 28:661–665
- Paton S (1992) Active normal faulting, drainage patterns and sedimentation in Southwestern Turkey. *J Geol Soc Lond* 149:1031–1044
- Petersen MD, Frankel AD, Harmsen SC, Mueller CS, Haller KM, Wheeler RL, Wesson RL, Zeng Y, Boyd OS, Perkins DM, Luco N, Field EH, Wills CJ, Rukstales KS (2008) Documentation for the 2008 update of the United States National Seismic Hazard Maps. US Geological Survey Open-File Report 2008-1128
- Petersen MD, Moschetti MP, Powers P, Mueller CS, Haller KM, Frankel AD, Zeng Y, Rezaeian S, Harmsen SC, Boyd OS, Field N, Chen R, Rukstales KS, Luco N, Wheeler RL (2014a) Updates to the 2014 US National seismic hazard maps: a summary of changes to seismic source and ground motion models. InL: Tenth US National conference on earthquake engineering, Anchorage, Alaska, July 21–25
- Petersen MD, Moschetti MP, Powers P, Mueller CS, Haller KM, Frankel AD, Zeng Y, Rezaeian S, Harmsen SC, Boyd OS, Field N, Chen R, Rukstales KS, Luco N, Wheeler RL, Williams RA, Olsen AH (2014b) Documentation for the 2014 Update of the United States National Seismic Hazard Maps. US Geological Survey Open-File Report 2014-1091. <http://dx.doi.org/10.333/ofr20141091/>
- Pucci S, De Martini PM, Pantosti D (2007) Preliminary slip rate estimates for the Düzce segment of the North Anatolian fault zone from offset geomorphic markers. *Geomorphology* 97(3–4):538–554
- Rangin C, Demirbağ E, İmren C, Crussion A, Normand A, Le Drezen E, Le Bot A (2001) Marine Atlas of the Sea of Marmara (Turkey). IFREMER, Paris. ISBN 2-84433-068-1
- Reilinger RE, McClusky SC, Oral MB, King W, Toksöz MN (1997) Global positioning, system measurements of present-day crustal movements in the Arabian–Africa–Eurasia plate collision zone. *J Geophys Res* 102:9983–9999
- Reilinger R, McClusky S, Vernant P, Lawrence S, Ergintav S, Cakmak R, Ozener H, Kadirov F, Guliev I, Stepanyan R, Nadariya M, Hahubia G, Mahmoud S, Sakr K, ArRajehi A, Paradissis D, Al-Aydrus A, Prilepin M, Guseva T, Evren E, Dmitrotsa A, Filikov SV, Gomez F, Al-Ghazzi R, Karam G (2006) GPS constraints on continental deformation in the Africa–Arabia–Eurasia continental collision zone and implications for the dynamics of plate interactions. *J Geophys Res* 111:B05411
- Rezaeian S, Petersen MD, Moschetti MP, Powers P, Harmsen SC, Frankel AD (2014) Implementation of NGA-West2 Ground Motion Models in the 2014 US National Seismic Hazard Maps. *Earthq Spectra* 30:1319–1333
- Robertson AHF (1998) Mesozoic–Tertiary tectonic evolution of the easternmost Mediterranean area: integration of marine and land evidence. In: Robertson AHF, Emeis K-C, Richter C (eds) Proceedings of ODP, Sci. Results 160. College Station, TX, pp 723–782
- Rockwell T, Ragona D, Seitz G, Langridge R, Aksoy ME, Uçarkuş G, Ferry M, Meltzner AJ, Klinger Y, Meghraoui M, Şatır D, Barka A, Akbalık B (2009) Paleoseismology of the North Anatolian Fault near the Marmara Sea: implications for fault segmentation and seismic hazard. In: Reicherter K, Michetti AM, Silva PG (eds) Paleoseismology: historical and prehistorical records of earthquake ground effects for seismic hazard assessment. The Geological Society, London, Special Publications, vol 316, pp 31–54
- Şaroğlu F (1985) Doğu Anadolu'nun neotektonik dönemde jeolojik ve yapısal evrimi. Doktora Tezi, İstanbul Üniv. Fen Bilimleri Enst. Jeol Müh Böl 240 s (Yayımlanmamış)
- Şaroğlu F, Güner Y (1981) Doğu Anadolu'nun jeomorfolojik gelişimine etki eden öğeler: jeomorfoloji, tektonik, volkanizma ilişkileri. *TJK Bül* 24:39–50
- Şaroğlu F, Yılmaz Y (1986) Doğu Anadolu'da neotektonik dönemdeki jeolojik evrim ve havza modelleri. *Min Res Expl Ist Turkey Bull* 115:43–52
- Şaroğlu F, Emre Ö, Boray A (1987) Türkiye'nin Diri Fayları ve Depremsellikleri. MTA Genel Müdürlüğü, Rapor no: 8174, 394 s., Ankara
- Şaroğlu F, Emre Ö, Kuşçu İ (1992a) Türkiye Diriy Fay Haritası. MTA Genel Müdürlüğü, Ankara
- Şaroğlu F, Emre Ö, Kuşçu İ (1992b) The East Anatolian Fault zone of Turkey. *Ann Tecton* 6:99–125
- Sato T, Kasahara J, Taymaz T, Ito M, Kamimura A, Hayakawa T, Tan O (2004) A study of microearthquake seismicity and focal mechanisms within the Sea of Marmara (NW Turkey) using ocean bottom seismometers. *Tectonophysics* 391:303–314

- Scholz CH (1982) Scaling laws for large earthquakes: consequences for physical models. *Bull Seism Soc Am* 72:1–14
- Seeber L, Emre O, Cormier M-H, Sorlien CC, McHugh CMG, Polonia A, Scientific Team of Marmara 2001 (2004) Uplift and subsidence from oblique slip: the Ganos-Marmara Bend of the North Anatolian Transform Western Turkey. *Tectonophysics* 391:239–258
- Şengör AMC (1979a) The North Anatolian transform fault: its age, offset and tectonic significance. *J Geol Soc Lond* 136:269–282
- Şengör AMC (1979b) Mid-Mesozoic closure of Permo-Triassic Tethys and its implications. *Nature* 279:590–593
- Şengör AMC (1980) Türkiye'nin neotektoniğinin esasları. Türkiye Jeolojisi Kurumu Yayınları
- Şengör AMC (1982) Ege'nin neotektonik evrimini yöneten etkenler. Türkiye Jeoloji Kurultayı, Batı Anadolu'nun Genç Tektoniği ve Volkanizması Paneli, Ankara, pp 59–71
- Şengör AMC (1987) Cross faults and differential stretching of hanging wall in regions of low-angle normal faulting: examples from western Turkey. In: Coward MP, Dewey JF, Hancock P (eds) *Continental extensional tectonics*, Geol Soc London, Special Publication 28:575–589
- Şengör AMC, Barka AA (1992) Evolution of escape-related strike-slip systems: implications for distribution of collisional orogens. In: 29th International geological congress, Kyoto, Japan, Abstracts 1, p 232
- Şengör AMC, Kid WSF (1979) Post-collisional tectonics of the Turkish-Iranian plateau and a comparison with Tibet. *Tectonophysics* 55:361–376
- Şengör AMC, Yılmaz Y (1981) Tethyan evolution of Turkey: a plate tectonic approach. *Tectonophysics* 75:181–241
- Şengör AMC, Görür N, Şaroğlu F (1985) Strike-slip faulting and related basin formation in zones of tectonic escape: Turkey as a case study. In: Biddle KT, Christie-Blick N (eds) *Strike-slip deformation, basin formation and sedimentation society of economic paleontologists and mineralogists special publication* 37:227–264
- Şengör AMC, Tuysuz O, İmren C, Sakinc M, Eyidogan H, Gorur G, Le Pichon X, Rangin C (2005) The North Anatolian fault: a new look. *Annu Rev Earth Planet Sci* 33:37–112
- Seyitoğlu G, Scott BC, Rundle CC (1992) Timing of Cenozoic extensional tectonics in west Turkey. *J Geol Soc Lond* 149:533–538
- Seymen İ, Aydın A (1972) Bingöl deprem fayı ve bunun Kuzey Anadolu Fayı ile olan ilişkisi. *Bull Gen Dir Miner Res Explor* 79:1–18
- Slemmons DB, Bodin P, Zang X (1989) Determination of earthquake size from surface faulting events. In: *Proceedings of the international seminar on seismic zonation*, Guangzhou, China, State Seismological Bureau, Beijing, 13
- Sözbilir H, Sümer Ö, Özkaymak Ç, Uzel B, Güler T, Eski S (2016) Kinematic analysis and palaeoseismology of the Edremit Fault Zone: evidence for past earthquakes in the southern branch of the North Anatolian fault zone, Biga Peninsula, NW Turkey. *Geodin Acta*. doi:[10.1080/09853111.2016.1175294](https://doi.org/10.1080/09853111.2016.1175294)
- Stein RS, Barka AA, Dieterich JH (1997a) Progressive failure on the North Anatolian fault since 1939 by earthquake stress triggering. *Geophys J Int* 128:594–604
- Stein RS, Barka AA, Dieterich JH (1997b) Progressive failure on the North Anatolian fault since 1939 by earthquake stress triggering. *Geophys J Int* 128:594–604
- Stirling MW, McVerry GH, Berryman KR (2002) A new seismic hazard model of New Zealand. *Bull. Seis. Soc. Am.* 92:1878–1903
- Stirling M, McVerry G, Gerstenberger M, Litchfield N, Van Dissen R, Berryman K, Barnes P, Wallace L, Villamor P, Langridge R, Lamarche G, Nodder S, Reyners M, Bradley B, Rhoades D, Smith W, Nicol A, Pettinga J, Clark K, Jacobs K (2012) National seismic hazard model for New Zealand: 2010 update. *Bull Seismol Soc Am* 102:1514–1542. doi:[10.1785/0120110170](https://doi.org/10.1785/0120110170)
- Sümer Ö, İnci U, Sözbilir H (2013) Tectonic evolution of the Söke Basin: extension-dominated transtensional basin formation in western part of the Büyük Menderes Graben, Western Anatolia, Turkey. *J Geodyn* 65:148–175
- Tan O (2012) The dense micro-earthquake activity at the boundary between the Anatolian and South Aegean microplates. *J Geodyn* 1160:19p
- Tatar O, Poyraz F, Gursoy H, Cakir Z, Ergintav S, Akpınar Z, Koçbulut F, Sezen F, Türk T, Hastaoğlu KÖ, Polat A, Mesci B, Gürsoy Ö, Ayazlı İE, Çakmak R, Belgen A, Yavaşoğlu H (2012) Crustal deformation and kinematics of the eastern part of The North Anatolian fault zone (Turkey) from GPS measurements. *Tectonophysics* 518–521:55–62
- Taymaz T, Price SP (1992) The 12.5 1971 Burdur earthquake sequence: a synthesis of seismological data and geological observations. *Geophys J Int* 108:589–603
- Taymaz T, Eyidoğan H, Jackson J (1991a) Source parameters of large earthquakes in the East Anatolian fault zone. *Geophys J Int* 106:537–550

- Taymaz T, Jackson J, McKenzie A (1991b) Active tectonics of the north and central Aegean Sea. *Geophys J Int* 106(2):433–490
- Taymaz T, Wright TJ, Soysal S, Tan O, Fielding E, Seyitoğlu G (2001) Source characteristics of the June 6 2000 Orta-Çankırı (central Turkey) earthquake: a synthesis of seismological, geological and geodetic (InSAR) observations, and internal deformation of the Anatolian plate. *Geol Soc Spec Publ* 291:259–290. doi:10.114/SP291.12
- Tezel T, Shibutani T, Kaypak B (2010) Crustal structure variation in western Turkey inferred from the receiver function analysis. *Tectonophysics* 492:240–252. doi:10.1016/j.tecto.2010.06.006
- Tiryakioğlu I, Floyd M, Erdogan S, Güllü E, Ergintav S (2013) GPS constraints on active deformation in the Isparta Angle region of SW Turkey. *Geophys J Int Adv Access* (published September 17, 2013)
- Tokay M (1973) Kuzey Anadolu Fay Zonunun Gerede ile İlgaz arasındaki kısmında jeolojik gözlemler. In: *Kuzey Anadolu Fayı ve Deprem Kuşağı Simpozyumu* (29–31 Mart 1972, Ankara), MTA. Enstitüsü, pp 12–29, Ankara
- Toksöz MN, Shakal AF, Michael AJ (1979) Space-time migration of earthquakes along the North Anatolian Fault zone and seismic gaps. *Pegeoph* 117:1258–1270
- Türkelli N et al (2003) Seismogenic zones in Eastern Turkey. *Geophys Res Lett* 30(24):8039. doi:10.1029/2003gl018023
- Ustaömer T, Gökaşan E, Tur H, Görüm T, Batuk FG, Kalafat D, Alp H, Ecevitöğlu B, Birkan H (2008) Faulting, mass-wasting and deposition in an active dextral shear zone, the Gulf of Saros and the NE Aegean Sea, NW Turkey. *Geo Mar Lett* 28:171–193. doi:10.1007/s00367-007-0099-6
- Utkucu M (2013) 23 October 2011 Van, Eastern Anatolia, earthquake (M (W) 7.1) and seismotectonics of Lake Van area. *J Seismol* 17:783–805. doi:10.1007/s10950-012-9354-z
- Vernant, Ph, Nilforoushan F, Hatzfeld D, Abbassi MR, Vigny C, Masson F, Nankali H, Martinod J, Ashtiani A, Bayer R, Tavakoli F, Chery J (2004) Present-Day crustal deformation and plate kinematics in the middle east constrained by gps measurements in Iran and Northern Oman. *Geophys J Int* 157:381–398
- Wells DL, Coppersmith KJ (1994) New empirical relationships among magnitude, rupture length, rupture width, rupture area, and surface displacement. *Bull Seismol Soc Am* 84:974–1002
- Wesnowsky S (2008) Displacement and geometrical characteristics of earthquake surface ruptures: issues and implications for seismic-hazard analysis and the process of earthquake rupture. *Bull Seismol Soc Am* 98(4):1609–1632. doi:10.1785/0120070111
- Westaway R (2003) Kinematics of the Middle East and eastern Mediterranean updated. *Turkish J Earth Sci* 12:5–46
- Westaway R (2004) Kinematic consistency between the Dead Sea Fault Zone and the Neogene and Quaternary left-lateral faulting in SE Turkey. *Tectonophysics* 391:203–237. doi:10.1016/j.tecto.2004.07.014
- Westaway R, Arger J (1996) The Gölbaşı basin, southeastern Turkey: a complex discontinuity in a major strike-slip fault zone. *J Geol Soc London* 153:729–744
- Woessner J, Dancu L, Giardini D, Crowley H, Cotton F, Grünthal G, Valensise G, Arvidsson R, Basili R, Demircioğlu MN, Hiemer S, Meletti C, Musson RW, Rovida AN, Sesetyan K, Stucchi M, the SHARE consortium (2015) The 2013 European Seismic Hazard Model: key components and results. *Earthq Eng, Bull.* doi:10.1007/s10518-015-9795-1
- Wright T, Fielding E, Parsons B, England P, Haynes M (2000) Source parameters of the 17 August 1999 İzmit earthquake from SAR interferometry. In: Barka AA, Kozacı O, Akyüz SH, Altunel E (eds) 1999 İzmit and Düzce Earthquakes: Preliminary Results, İstanbul Technical University Publ, pp 289–293, İstanbul
- Yavasoglu H, Tari E, Tüysüz B, Çakır Z, Ergintav S (2011) Determining and modelling tectonic movements along the central part of the North Anatolian Fault (Turkey) using geodetic measurements. *J Geodyn* 51:339–343
- Yiğitbaş E, Yılmaz Y (1996) Post-Late Cretaceous strike-slip tectonics and its implications for the Southeast Anatolian Orogen, Turkey. *Int Geol Rev* 38(1996):818–831
- Yılmaz Y (1993) New evidence and model on the evolution of the Southeast Anatolian Orogen. *Geol Soc Am Bull* 105:251–271. doi:10.1130/0016-7606(1993)105<0251:Neamot>2.3.Co;2
- Yılmaz Y, Yiğitbaş E, Genç ŞC (1993) Ophiolitic assemblages and metamorphic of southeast Anatolia and their significance in the geological evaluation of the orogenic belt. *Tectonics* 12:1280–1297
- Yılmaz Y, Güner Y, Şaroğlu F (1998) Geology of the Quaternary volcanic centers of the east Anatolia. *J Volcanol Geotherm Res* 85:173–210
- Yılmaz Y, Genç ŞC, Güner F, Bozcu M, Karacık Z, Altunkaynak Ş, Elmas A (2000) When did the western Anatolian grabens begin to develop? In: E Bozkurt, JA Winchester, JDA Piper (eds) *Tectonics and magmatism in Turkey and surroundings area*, Geological Society of London, Special Publication No:173, pp 353–384

- Yolsal-Çevikbilen S, Biryol CB, Beck S, Zandt G, Taymaz T, Adıyaman HE, Özacar AA (2012) 3-D crustal structure along the North Anatolian fault zone in north-central Anatolia revealed by local earthquake tomography. *Geophys J Int* 188:819–849. doi:[10.1111/j.1365-246X.2011.05313.x](https://doi.org/10.1111/j.1365-246X.2011.05313.x)
- Yönlü Ö (2012) Late Quaternary Activity of the East Anatolian Fault Zone between Gölbaşı (Adıyaman) and Karataş (Adana). Doctoral Dissertation, Eskişehir Osmangazi University, Department of Geological Engineering (unpublished)
- Yönlü Ö, Altunel E, Karabacak V, Akyüz HS, Yalçın Ç (2010) Offset archaeological relics in the western part of the Büyük Menderes graben (western Turkey) and their tectonic implication. In: Sintubin M, Stewart IS, Niemi TM, Altunel E (eds) *Ancient Earthquakes: Geological Society of America, Special Paper 471*:269–279
- Zhu L, Akyol N, Mitchell J, Sozbilir H (2006) Seismotectonics of Western Turkey from high resolution earthquake relocations and moment tensor determinations. *Geophys Res Lett* 33:L07316. doi:[10.1029/2006GL025842](https://doi.org/10.1029/2006GL025842)
- Zor E, Sandvol E, Gürbüz C, Türkelli N, Seber D, Barazangi M (2003) The crustal structure of the East Anatolian plateau (Turkey) from receiver functions. *Geophys Res Lett* 30(24):8044. doi:[10.1029/2003GL018192](https://doi.org/10.1029/2003GL018192)